Astroparticle Physics with the GRAPES-3 Experiment

(Gamma Ray Astronomy at Pev Energies Phase-3)

(An India-Japan Collaboration)

ICCGF-2009, IIT Kanpur, 30 October 09

S.K. Gupta, H.M. Antia, S.R. Dugad, U.D. Goswami, A. Iyer, P. Jagadeesan, A. Jain, S. P.K. Mohanty, P.K. Nayak, B.S. Rao, K.C. Ravindran, S.C. Tonwar, Y. Hayashi, N. Ito, S. Kawakami, T. Matsuyama, M. Minamino, H. Kojima, S. Shibata, R. Koul, T.A. Mir, S. Mufti, S.K. Ghosh, P. Joarder, S. Raha, S. Saha, P. Subramanian, P. Jain, A. Oshima, H. Tanaka

1. Tata Institute of Fundamental Research, Mumbai, India
2. Osaka City University, Osaka, Japan
3. Aichi Institute of Technology, Toyota City, Japan
4. Bhabha Atomic Research Centre, Mumbai, India
5. Acharya J.C. Bose Institute, Kolkata, India
6. Indian Institute of Science and Engineering Research, Pune, India
7. Indian Institute of Technology, Kanpur, India
8. National Astronomical Observatory of Japan, Tokyo, Japan
9. IPMU, University of Tokyo, Tokyo, Japan

GRAPES-3 Scientific Objectives:

1. The origin, acceleration and propagation of UHE (>10^{14}eV) particles in the galaxy and beyond through the study of the "Knee" in energy spectrum and the nuclear composition.

2. Production and/or acceleration of highest energy (~10^{20}eV) particles in cosmic rays through the study of diffuse γ-rays of >100 TeV.

3. Astronomy at multi-TeV using γ-rays from neutron stars and other compact objects.

4. Sun the closest astrophysical source and accelerator of energetic particles and its effects on the Earth.

`knee' Region

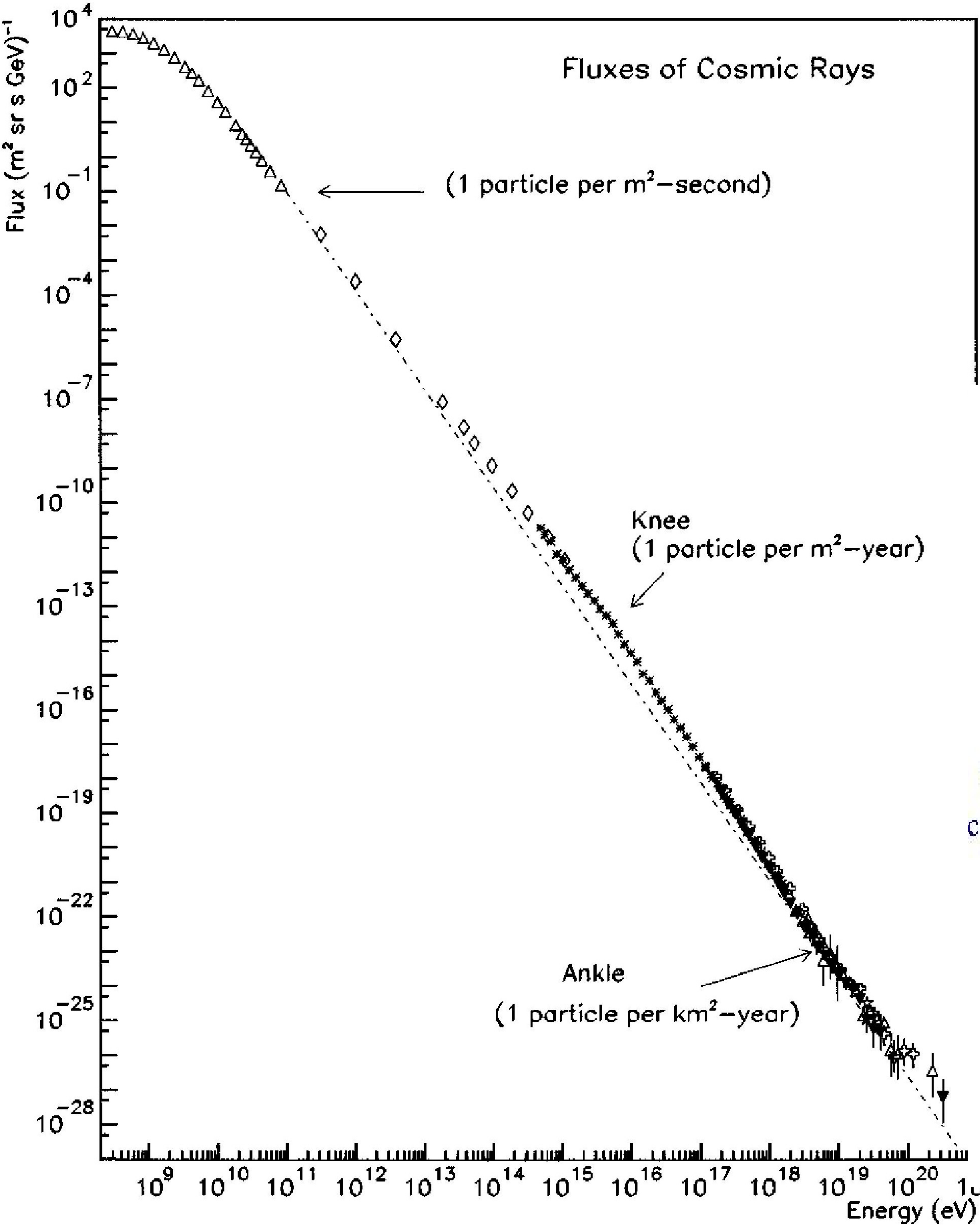
Fluxes of Cosmic Rays
Flux (m² sr s GeV)⁻¹
(1 particle per m²–second)
Knee
(1 particle per m²–year)
Ankle
(1 particle per km²–year)
Energy (eV)

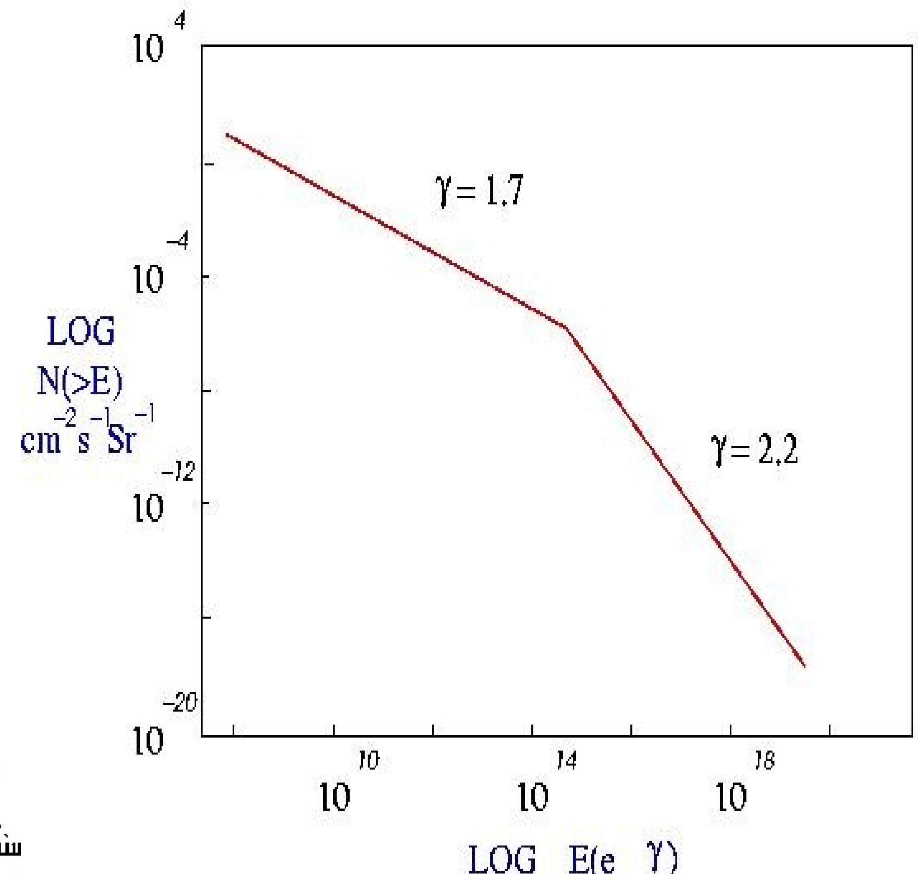
γ = 1.7
γ = 2.2
LOG N(>E) cm⁻² s⁻¹ Sr⁻¹
LOG E(eV)

Detection and Measurement of Cosmic Rays:

HE particles produce a shower of electromagnetic (e^+, e^-, γ) particles, muons (μ^+, μ^-) and other particles in atmosphere.

Measurement of particle density and time (ns) in the shower provides an estimate of the energy and direction of primary particle.

Measurement of muon density in the shower provides information on the composition of primary particle. It also allows discrimination between γ–rays and protons.

The flux of muons is sensitive to the solar wind and is used to study various Sun induced phenomena.

GRAPES-3: A powerful tool for Astroparticle Physics.

Conventional array with highest density of detectors

Basic Detector Component:

>400 - Plastic Scintillator detectors (1 m^2 area)

3712 - Proportional Counters (6m x 0.1m x 0.1m) deployed in four crossed layer configuration as 1 GeV muon detector of area 560 m^2.

© 2007 Europa Technologies
Image © 2007 DigitalGlobe
©2007 Google™
298 ft
Pointer 11°23'25.54" N 76°39'49.48" E elev 7223 ft
Streaming |||||||||| 100%
Eye alt 8167 ft


278
223
224
222


114
113
112
073

Detector Development: Plastic Scintillator

Decay Time= 1.6 ns

Light Output = 85% of Bicron (54% of anthracene)

Timing 25% faster than Bicron

Atten. Length λ= 100cm

Cost ~10% of Bicron

Size 50cmX50cm

Total > 1500

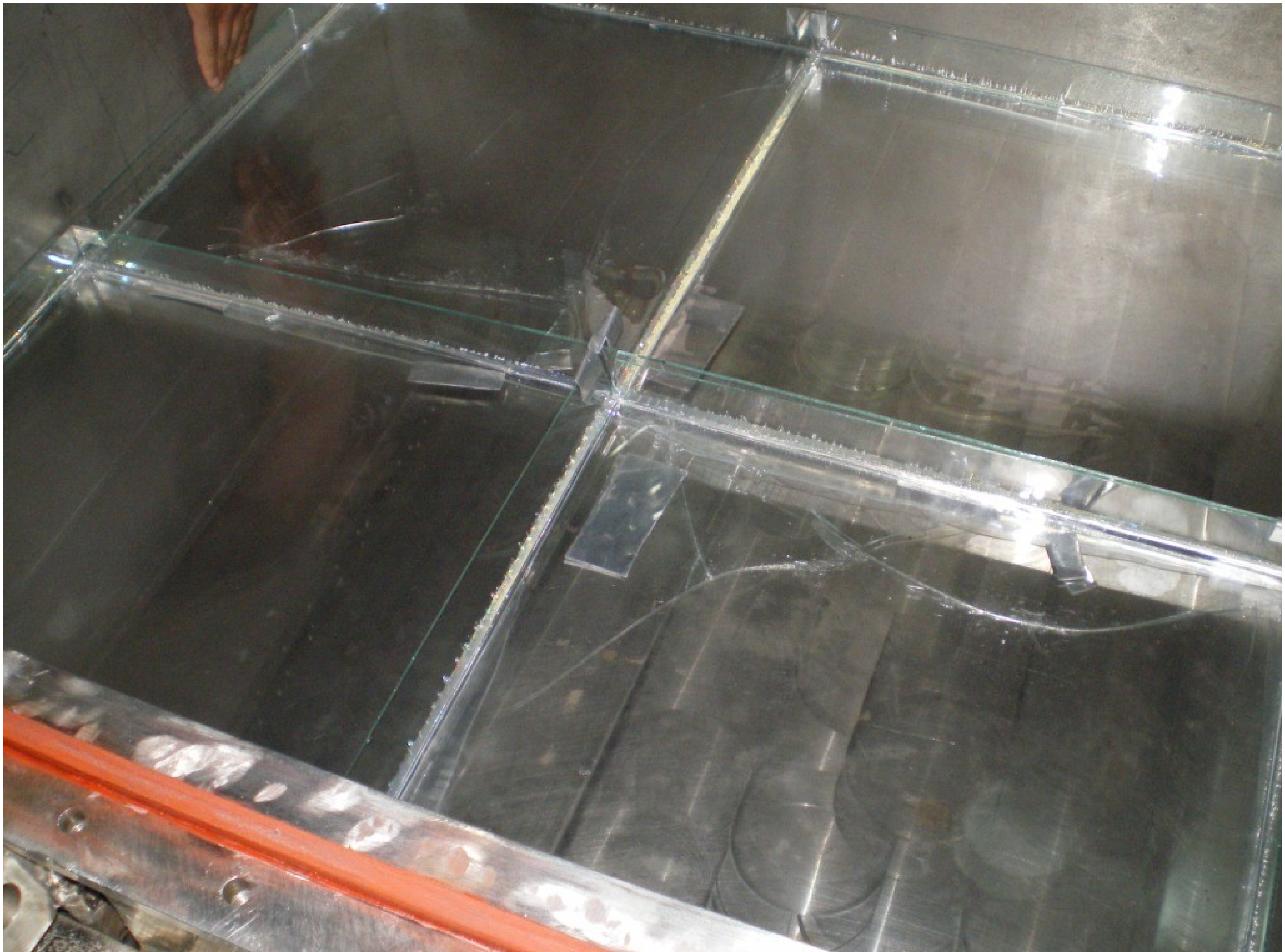


15

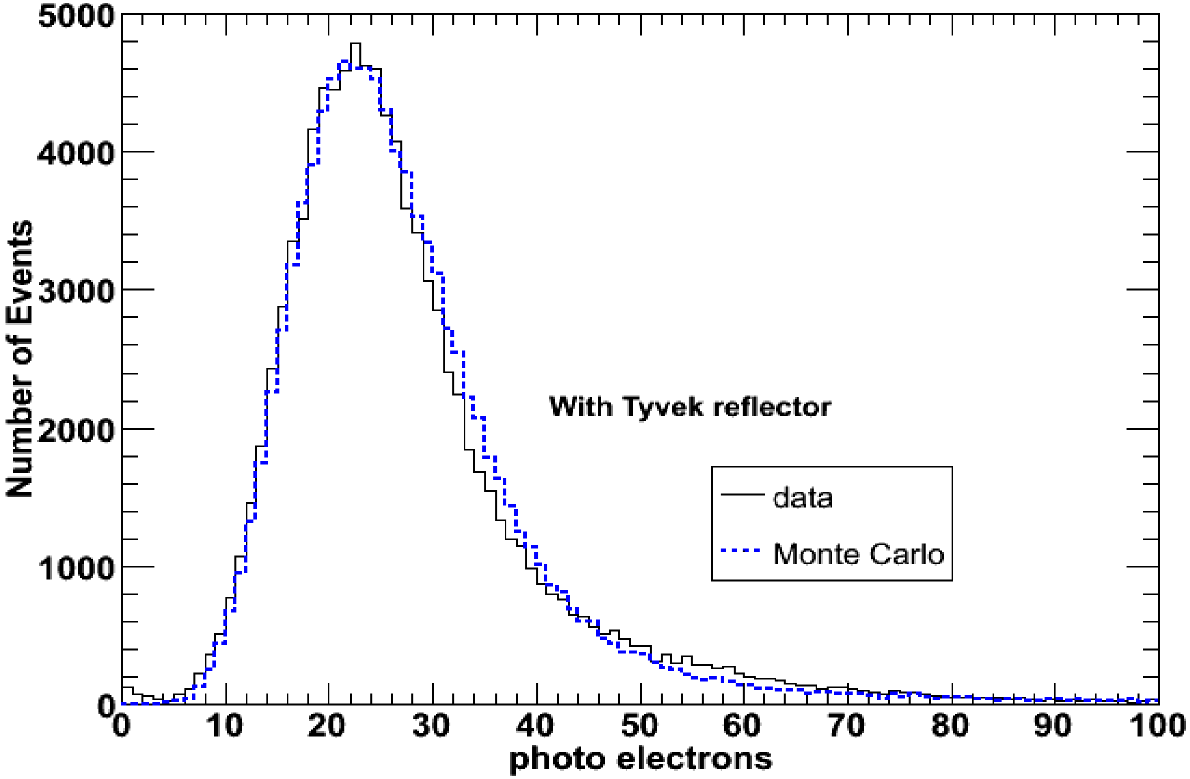

Number of Events
5000
4000
3000
2000
1000
0
0
10
20
30
40
50
60
70
80
90
100
photo electrons
With Tyvek reflector
data
Monte Carlo

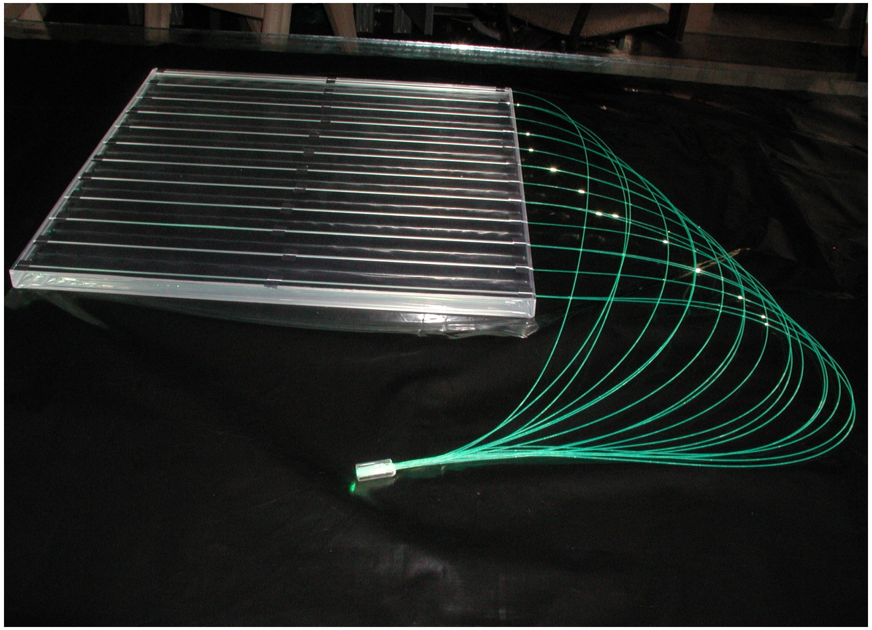

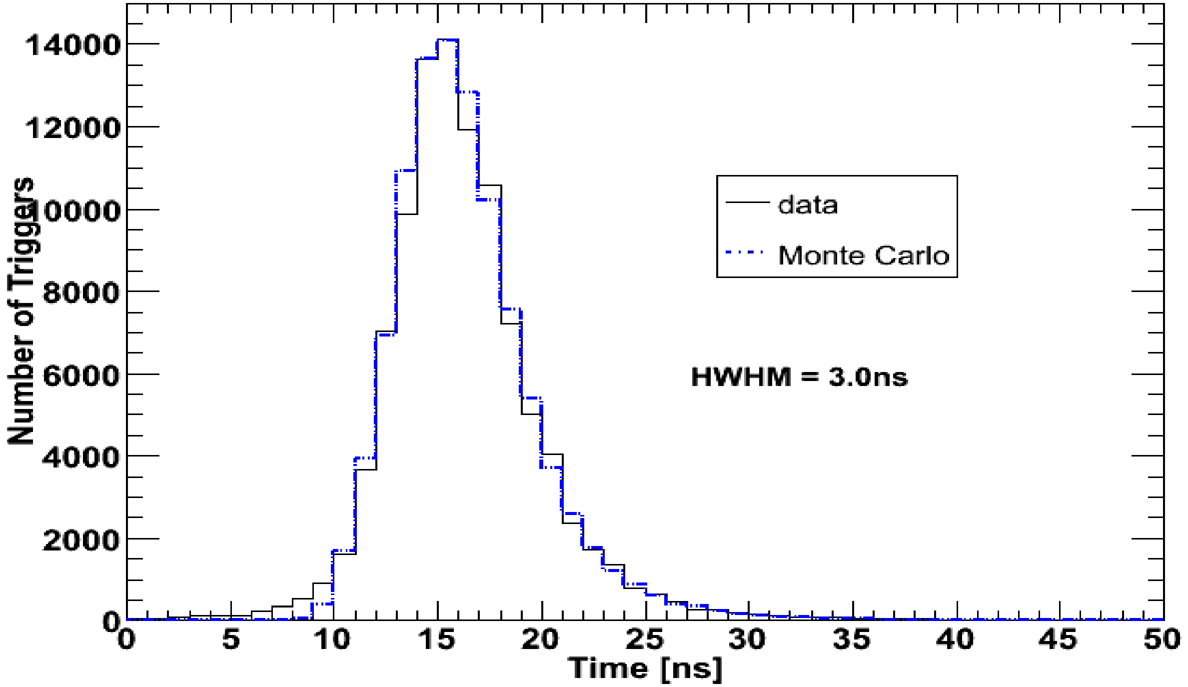

Number of Triggers
14000
12000
10000
8000
6000
4000
2000
0
0
5
10
15
20
25
30
35
40
45
50
Time [ns]
data
Monte Carlo
HWHM = 3.0ns

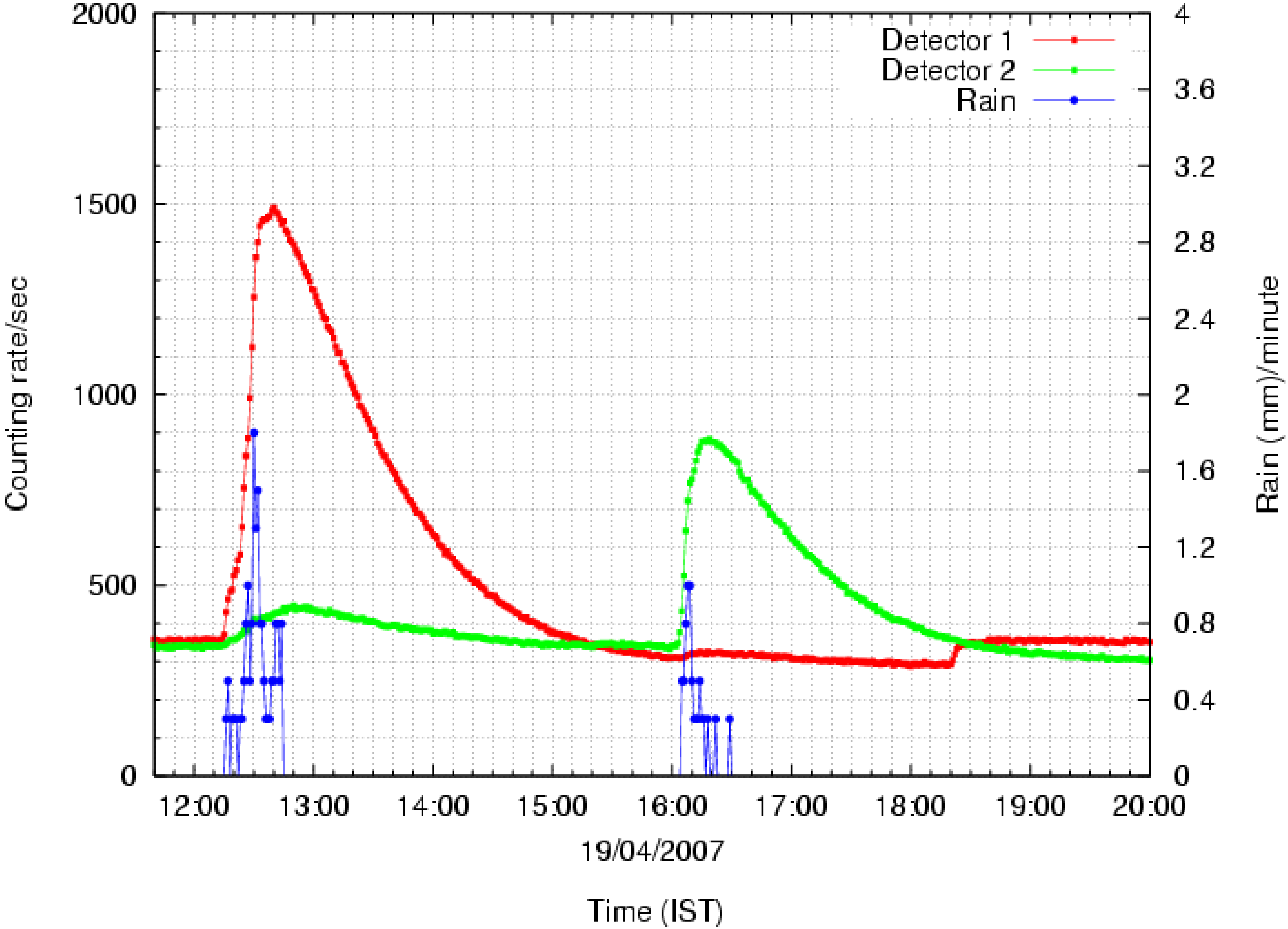

Detector 1
Detector 2
Rain
Counting rate/sec
Rain (mm)/minute
2000
1500
1000
500
0
4
3.6
3.2
2.8
2.4
2
1.6
1.2
0.8
0.4
0
12:00
13:00
14:00
15:00
16:00
17:00
18:00
19:00
20:00
19/04/2007
Time (IST)

Our requirement: Large number of channels for Signal Processing

Fast Amplifiers with >300 MHz bandwidth

+

Fast Discriminators with <100 ps time jitter

Charge integrating ADCs ≥12 bit dynamic range, fast conversion

Arrival time measurement by TDCs ≥12 bit dynamic range, 100 ps resolution, multi-hit capability, triggered operation

Amplifier-Discriminator response using muons

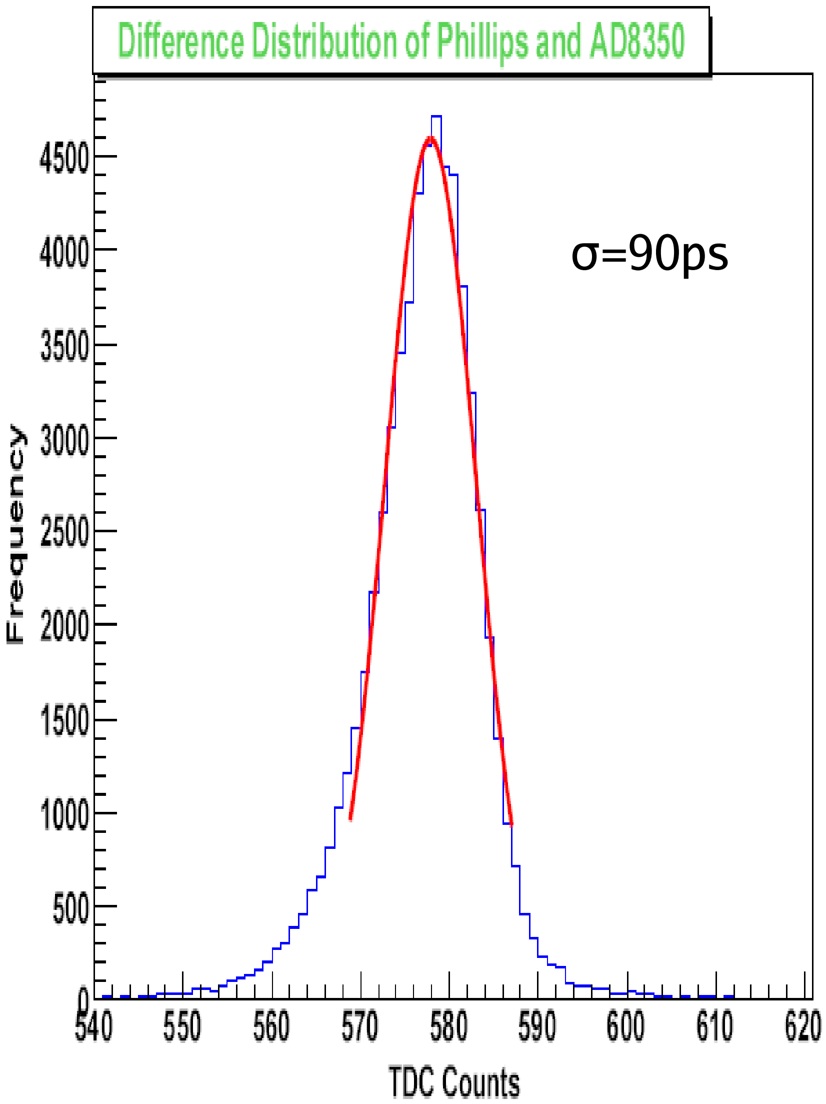

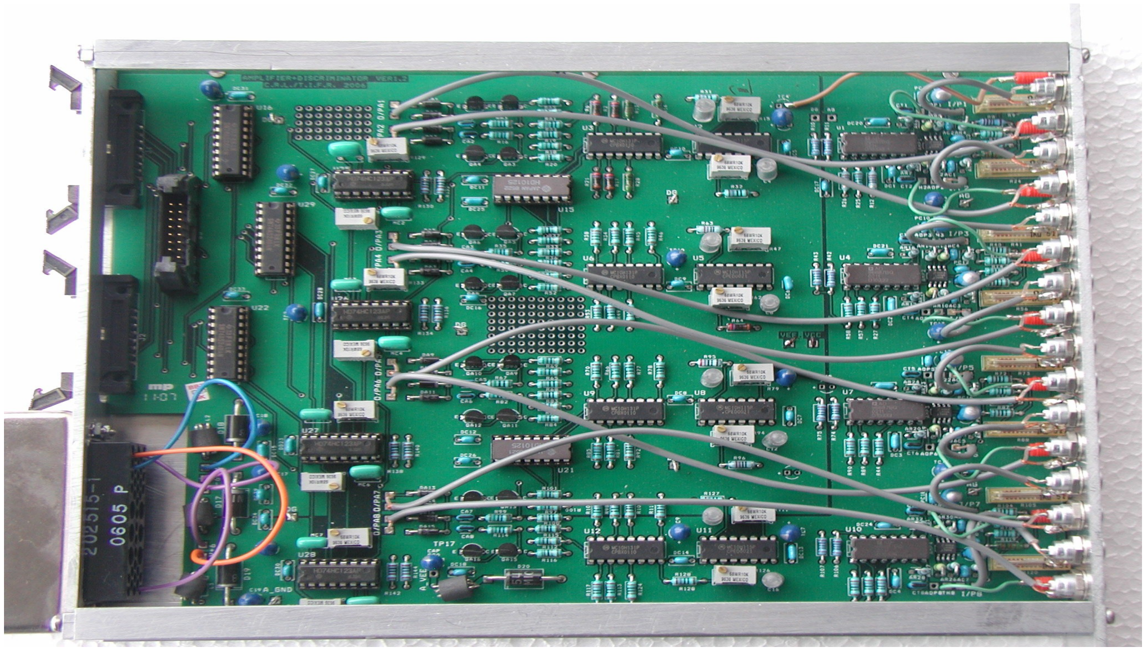

Performance of HPTDC

32 Channels
100 ps least count
Multi-hit capability
Huge dynamic range (100 ps - 50 μs)
Trigger mode (avoids delay cables)

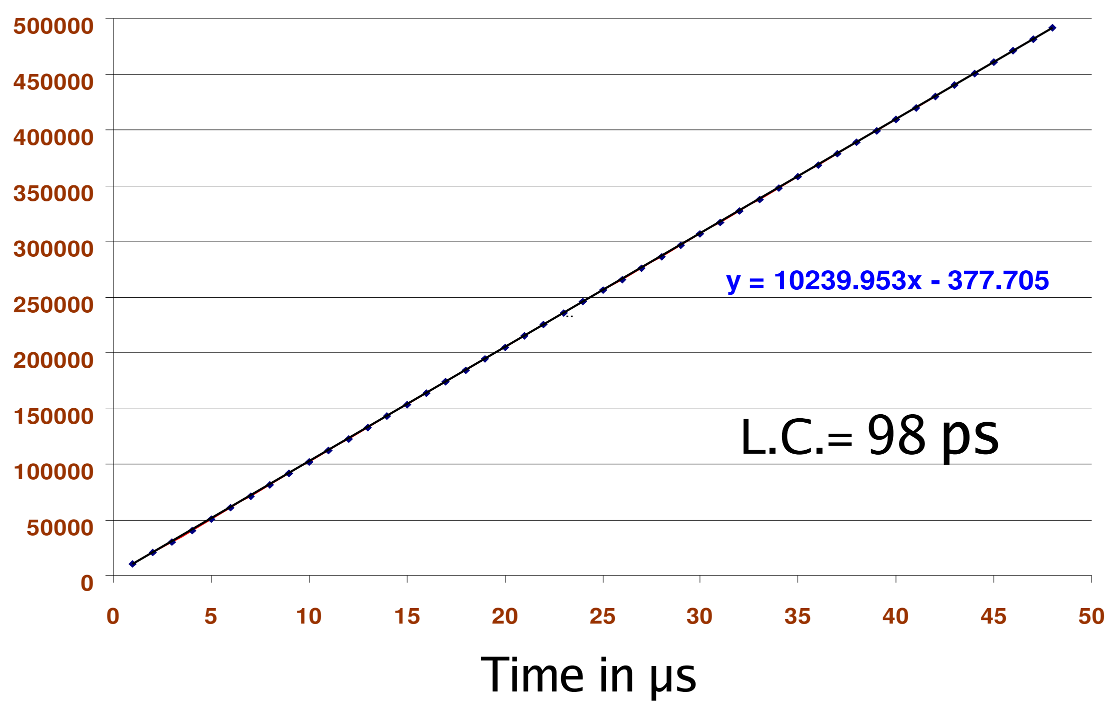

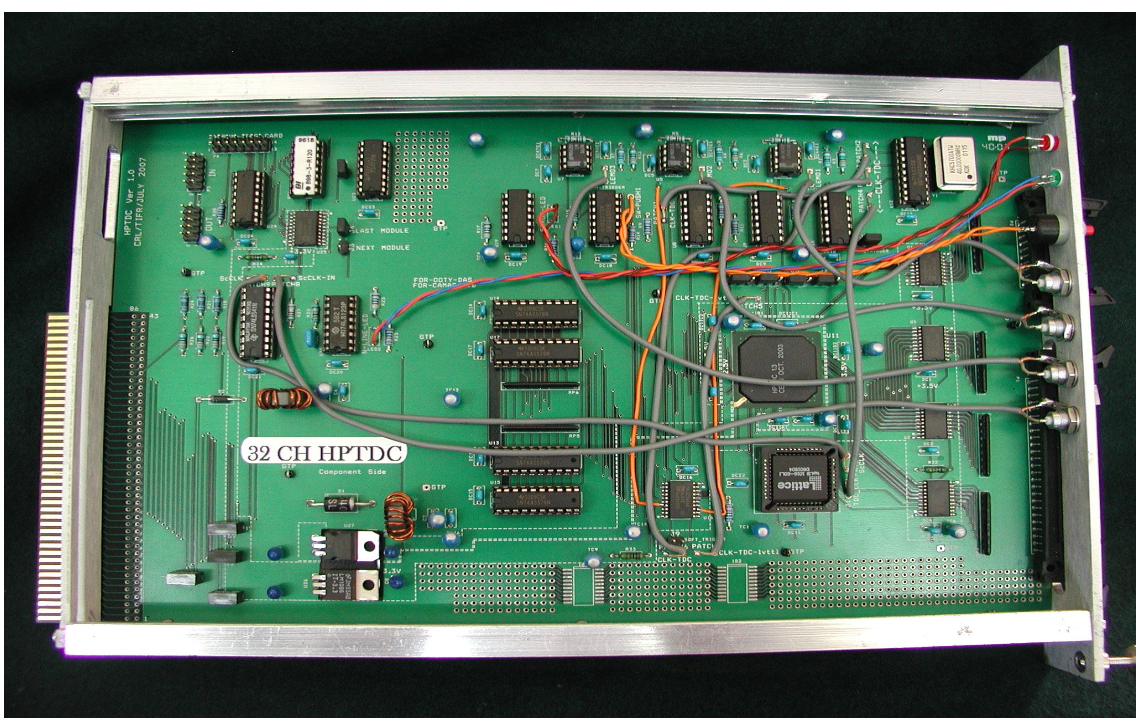

SiPM

- 5 nos of SiPM (Made in Russia)
- 5 nos of Pre-Amplifier boards (NE5539)
- 900 pixels (30x30 matrix) covering an area of $1mm^2$
- Photon Detection Efficiency ~35%
- Operating Voltage ~ 50 - 58 Volts (SRD)

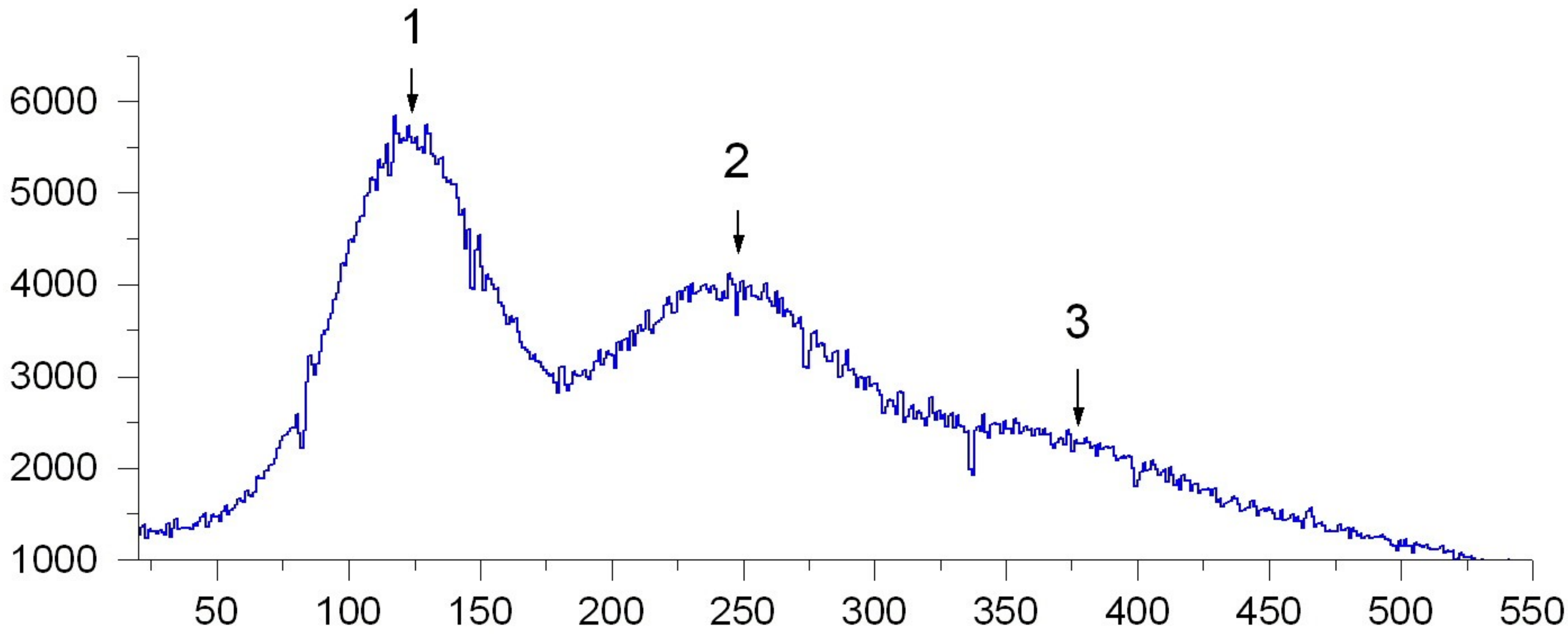
1
2
3
6000
5000
4000
3000
2000
1000
50
100
150
200
250
300
350
400
450
500
550

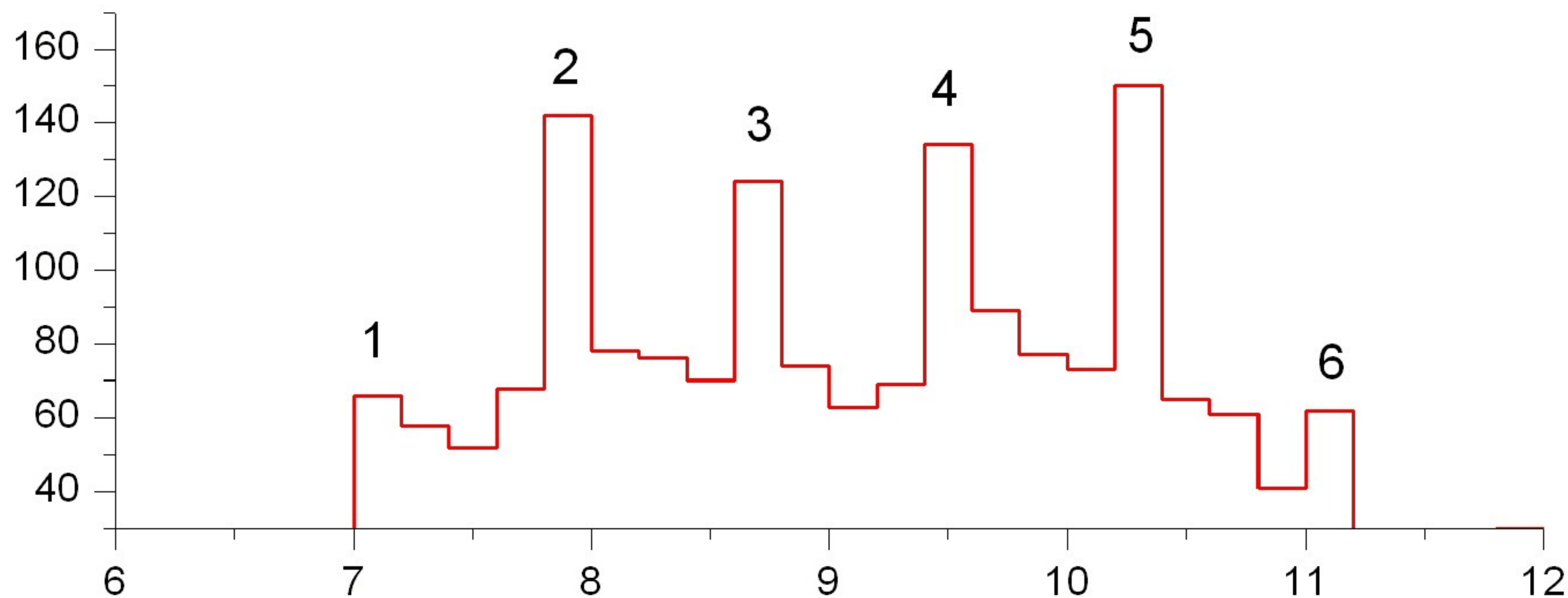
1
2
3
4
5
6
160
140
120
100
80
60
40
6
7
8
9
10
11
12

(a) Shower Size `N_e' $10^{4.4}$-$10^{4.6}$

(b) Shower Size `N_e' $10^{5.0}$-$10^{5.2}$

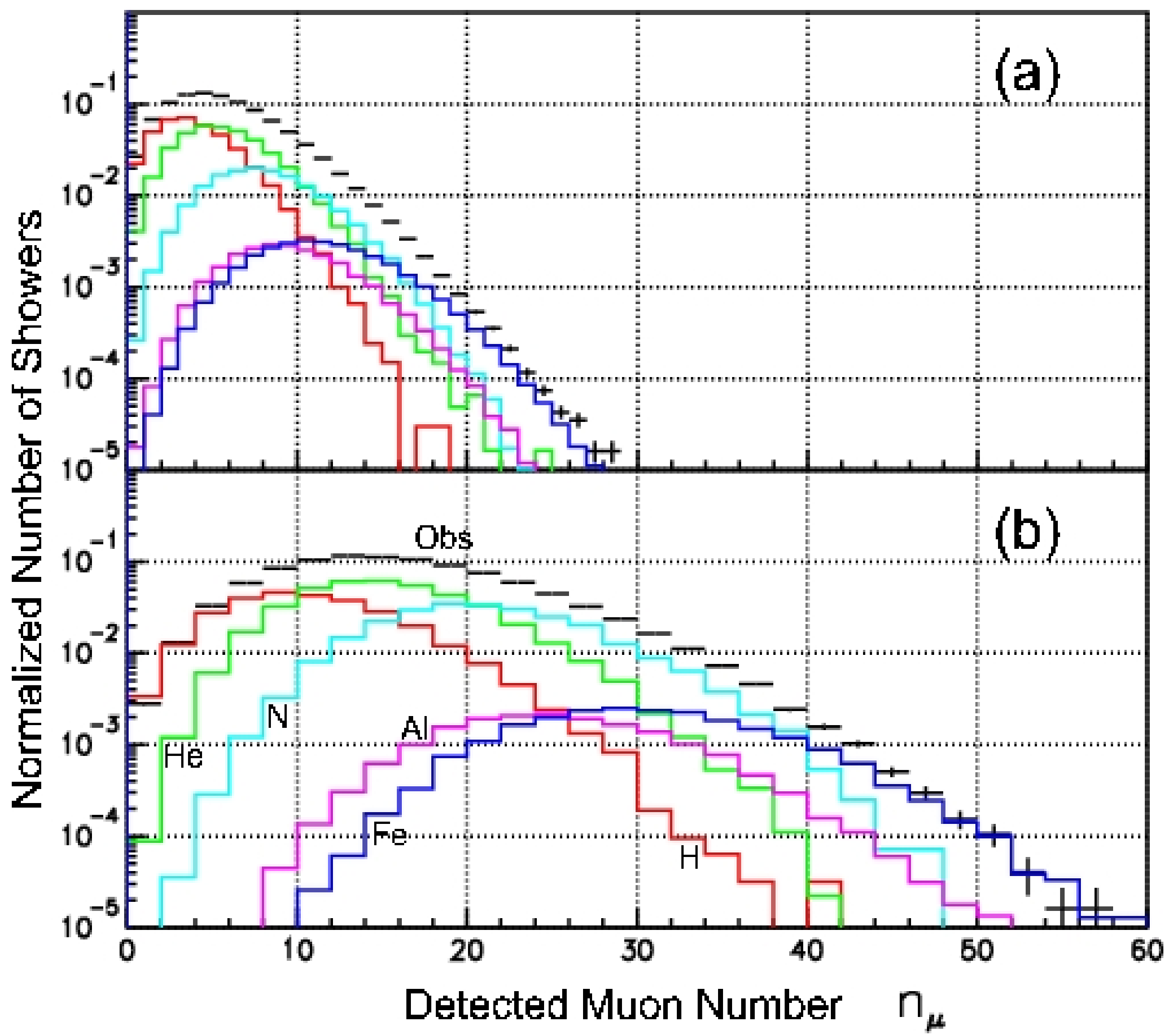

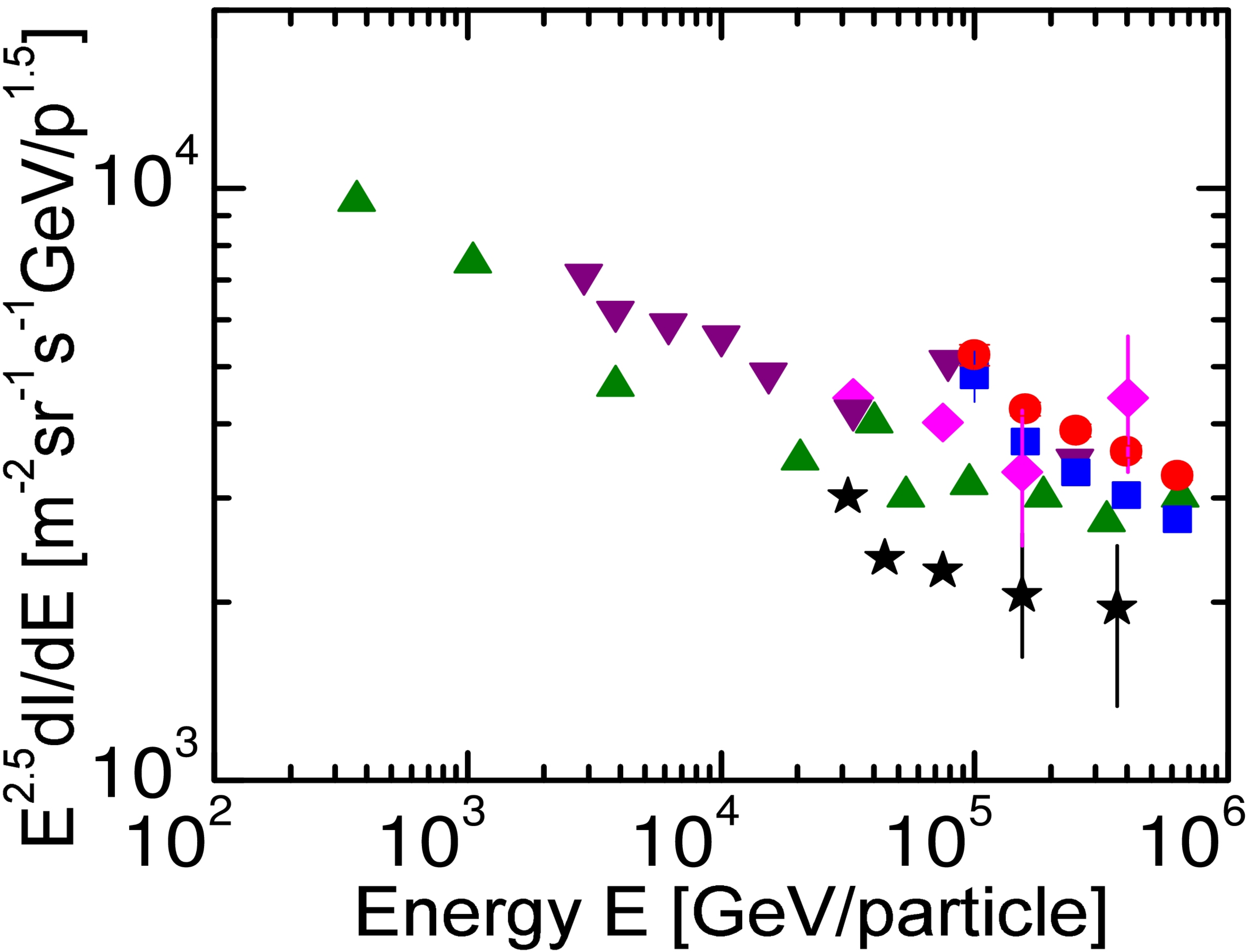

$E^{2.5}dI/dE$ [$m^{-2}sr^{-1}s^{-1}GeV/p^{1.5}$]
10^4
10^3
10^2
10^3
10^4
10^5
10^6
Energy E [GeV/particle]

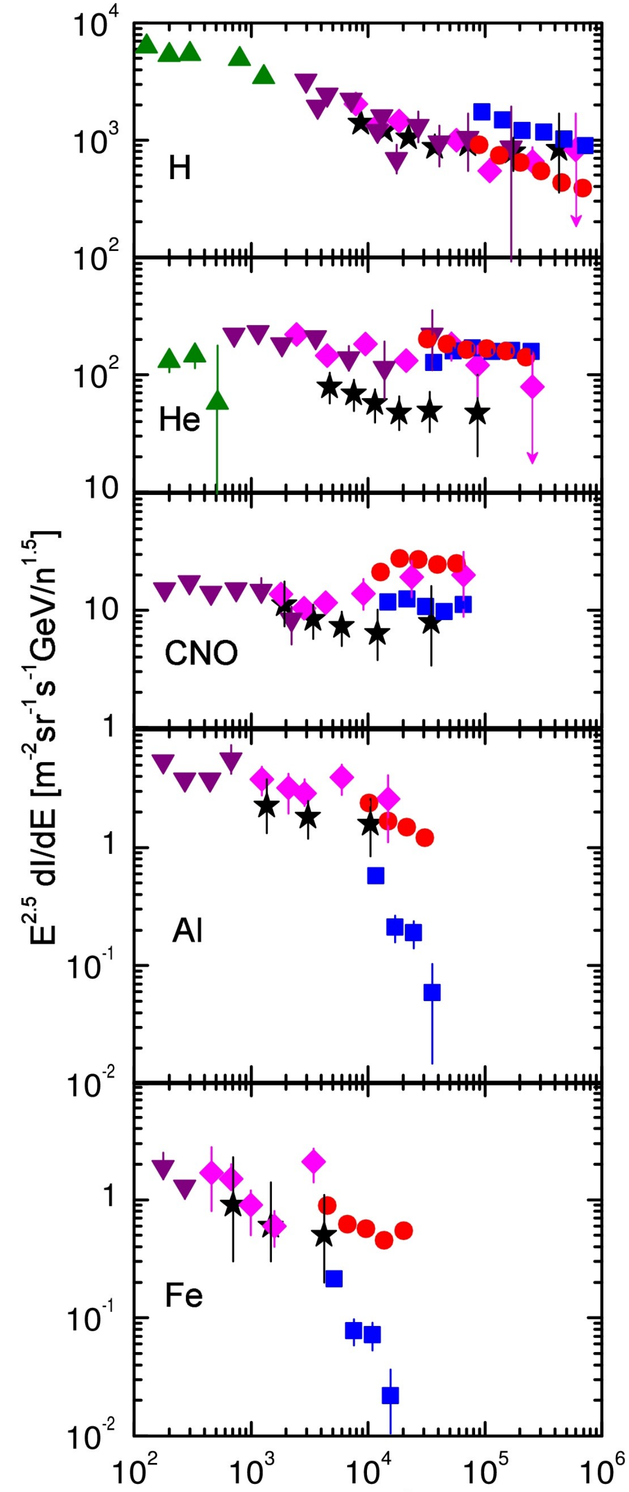

H
He
CNO
Al
Fe
E^2.5 dI/dE [m^-2 sr^-1 s^-1 GeV/n^1.5]
Energy E [GeV/n]

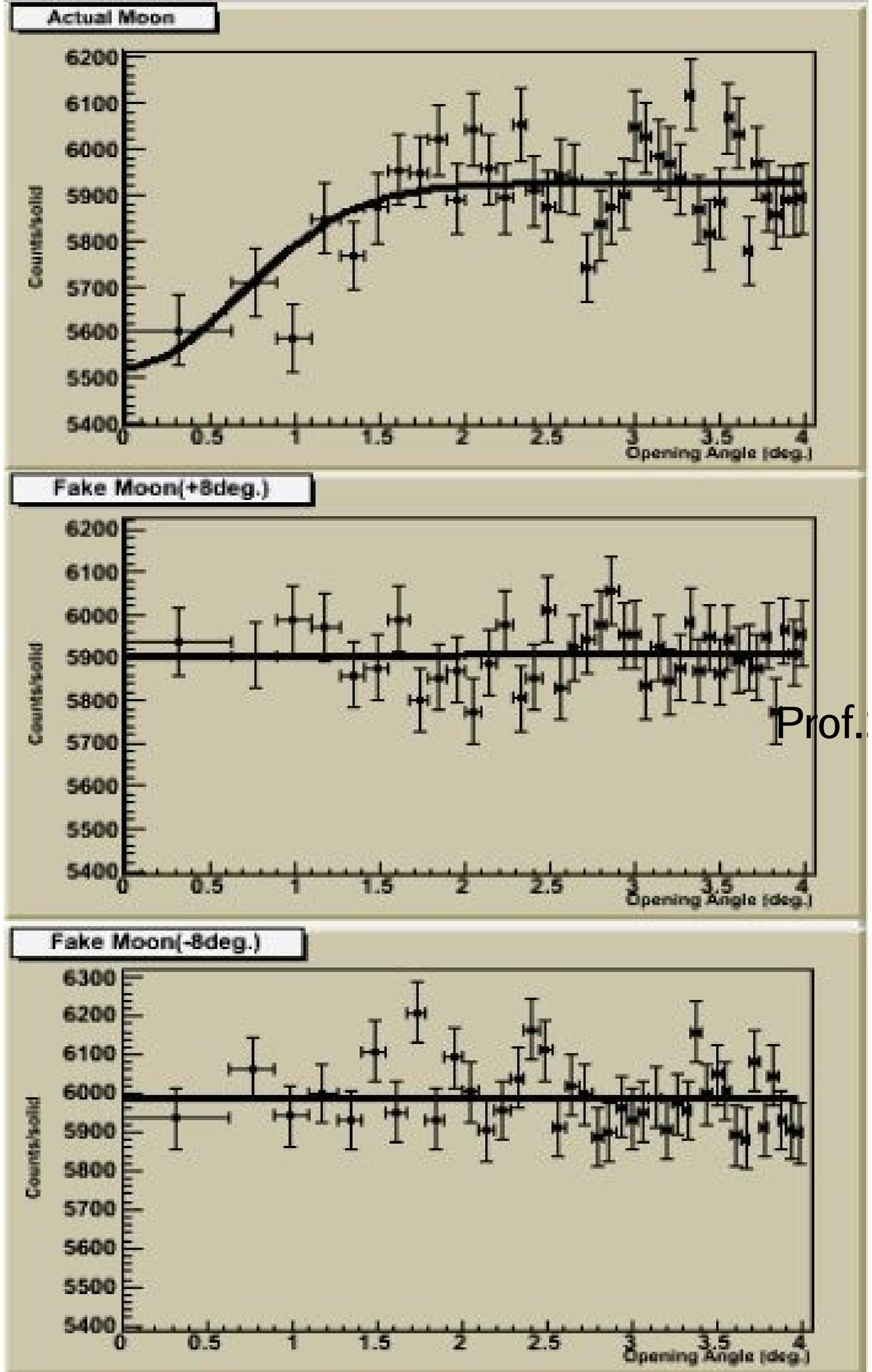

- γ-ray astronomy
- $\sigma_\theta = 0.5^o$ Moon Shadow

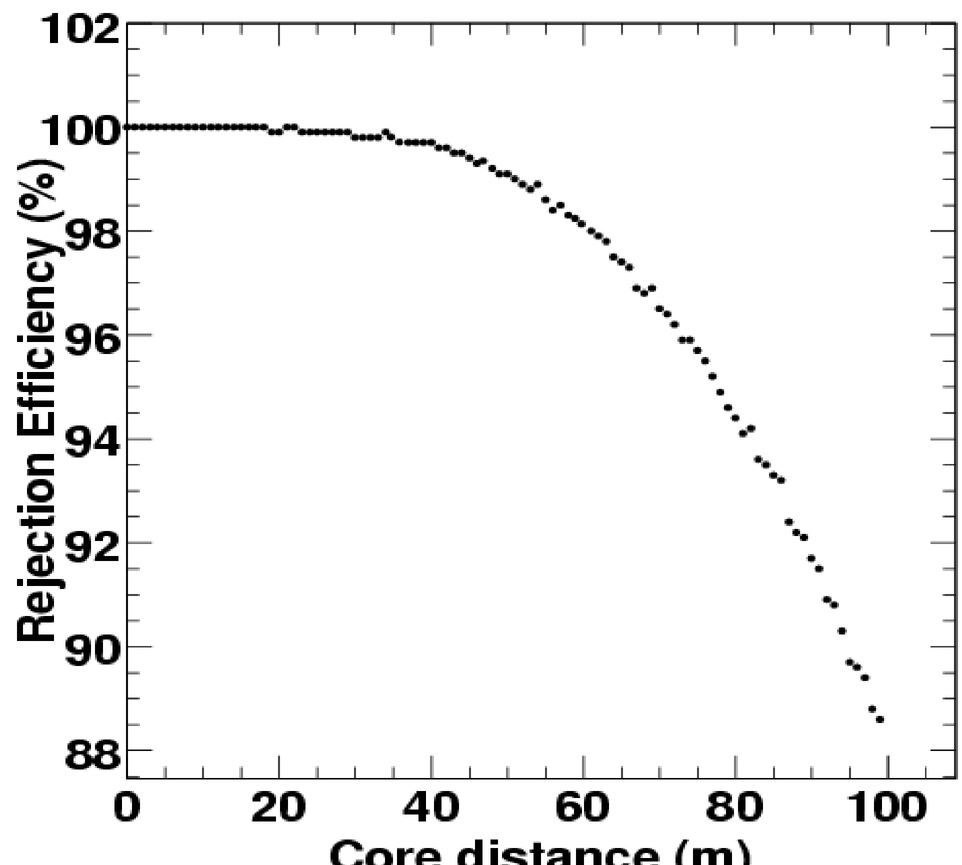

Moon and Sun shadow

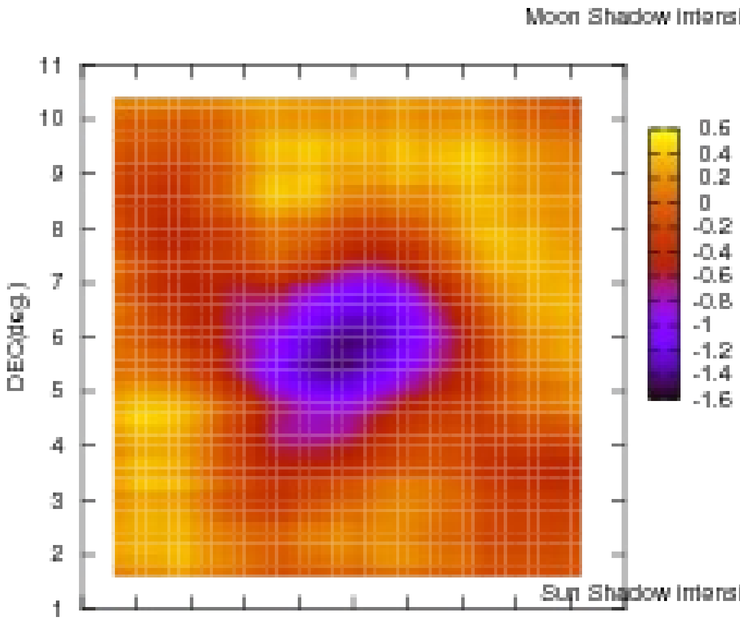

Moon

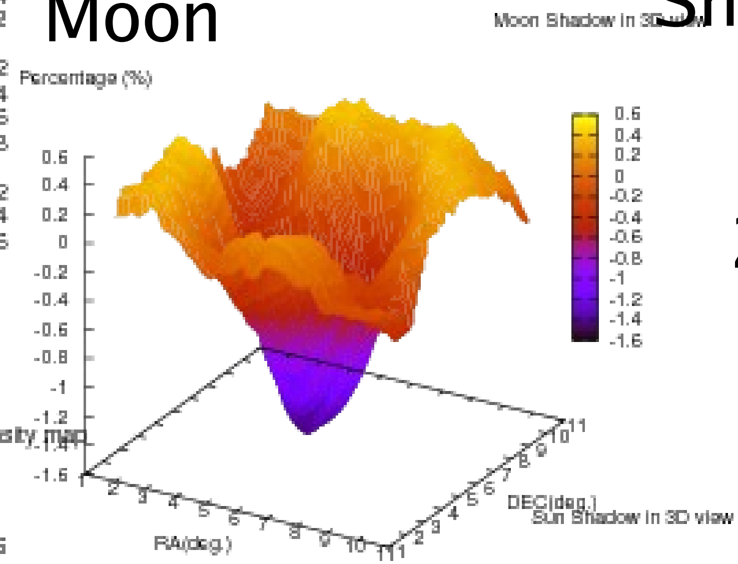

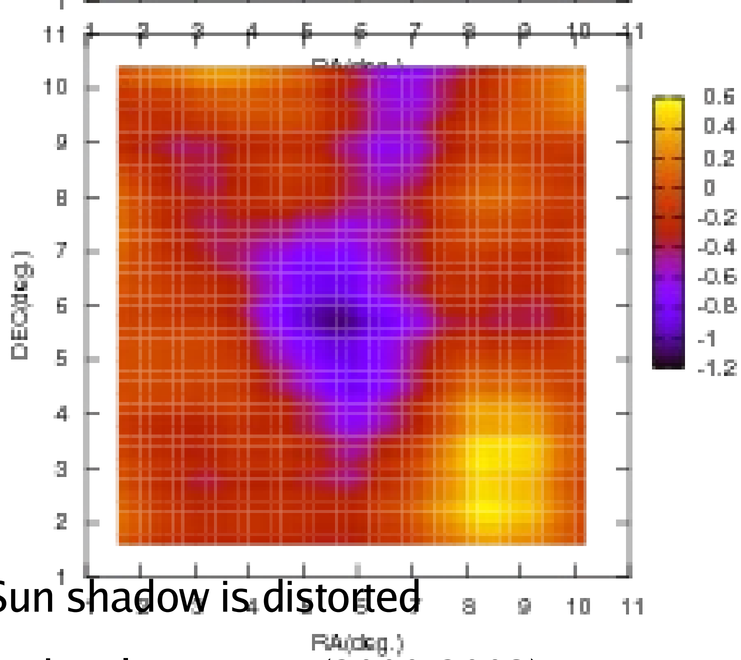

Sun

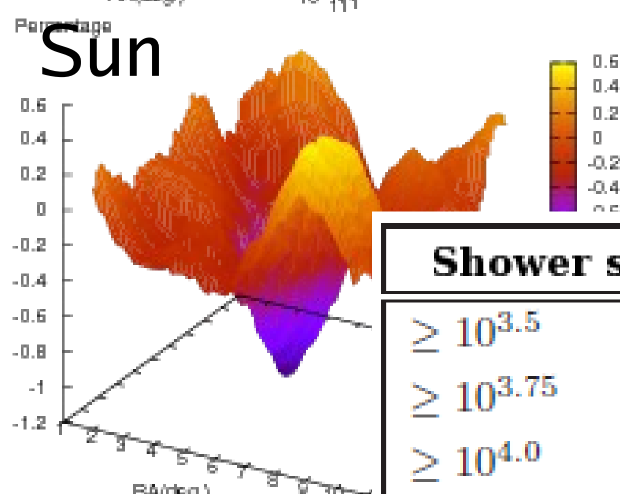

Sun shadow is distorted

High solar activity (2000-2003)

Shape of the shadow

↓

2D Gaussian

↓

Angular resolution Moon shadow

Shower size (N_e)	Ang. resolution	Error
$\geq 10^{3.5}$	1.07°	0.13°
$\geq 10^{3.75}$	0.89°	0.12°
$\geq 10^{4.0}$	0.73°	0.10°
$\geq 10^{4.25}$	0.61°	0.09°
$\geq 10^{4.5}$	0.50°	0.10°

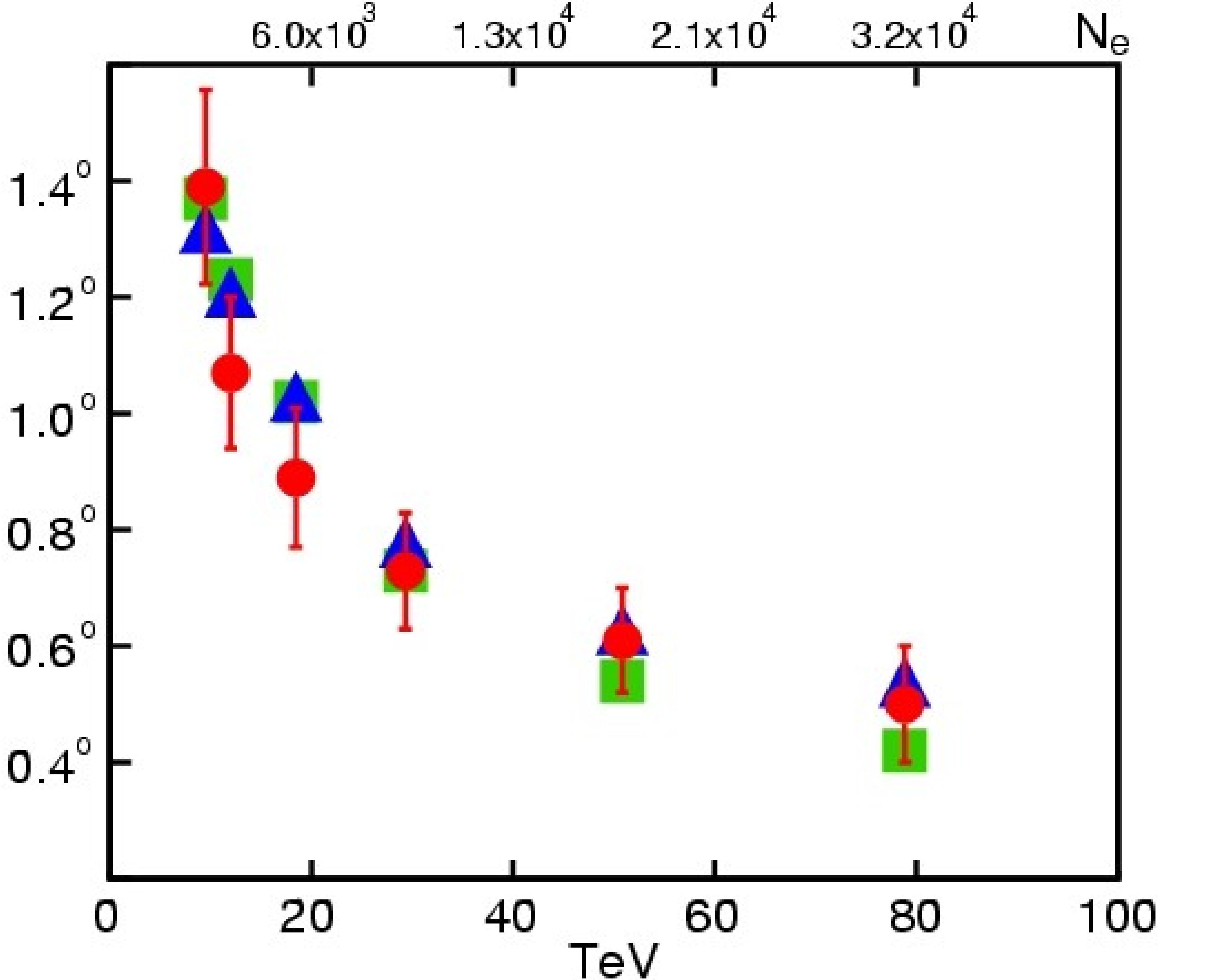

6.0x10^3
1.3x10^4
2.1x10^4
3.2x10^4
N_e
1.4°
1.2°
1.0°
0.8°
0.6°
0.4°
0
20
40
60
80
100
TeV

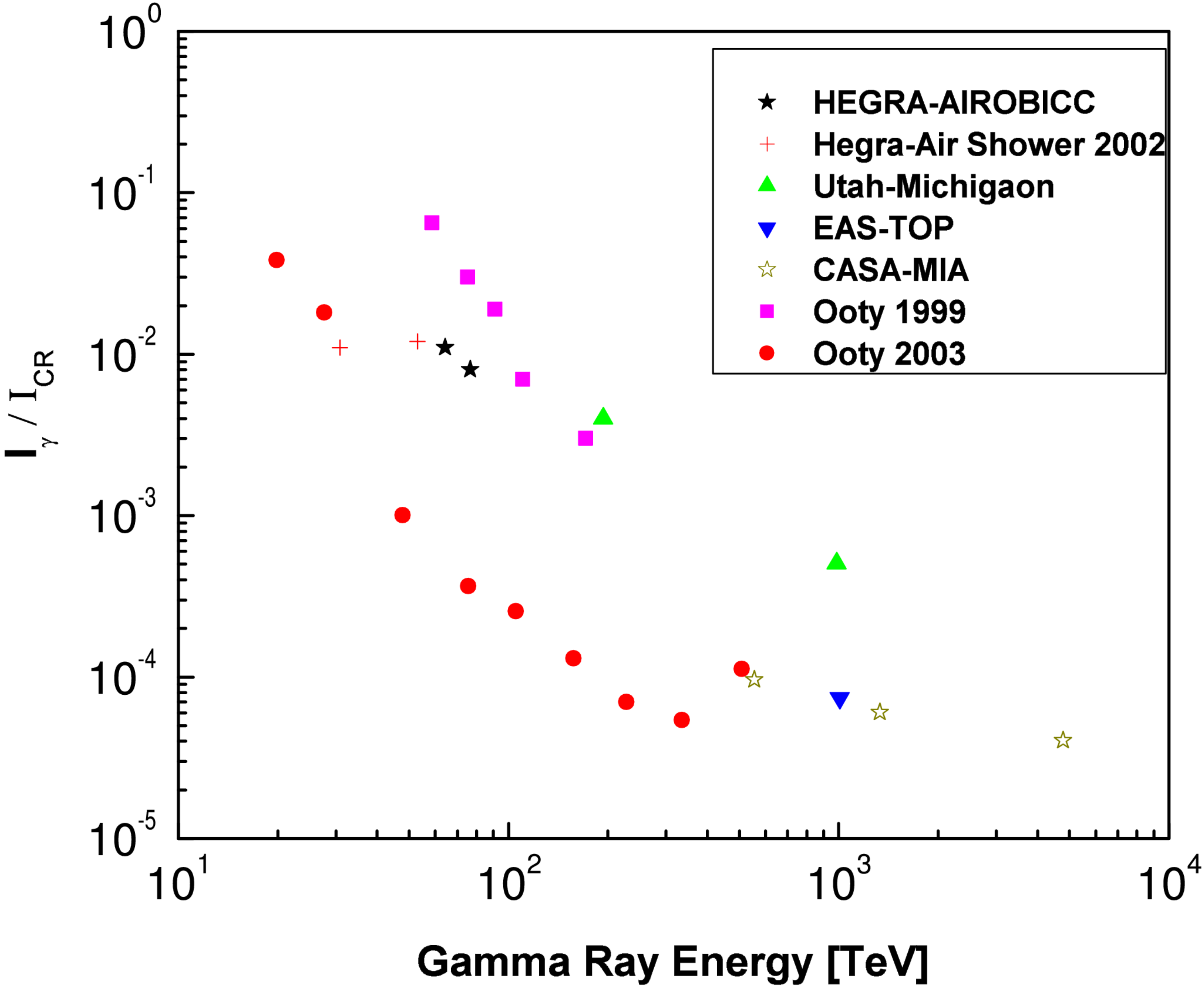

HEGRA-AIROBICC
Hegra-Air Shower 2002
Utah-Michigaon
EAS-TOP
CASA-MIA
Ooty 1999
Ooty 2003
10^0
10^{-1}
10^{-2}
10^{-3}
10^{-4}
10^{-5}
I_γ / I_{CR}
10^1
10^2
10^3
10^4
Gamma Ray Energy [TeV]

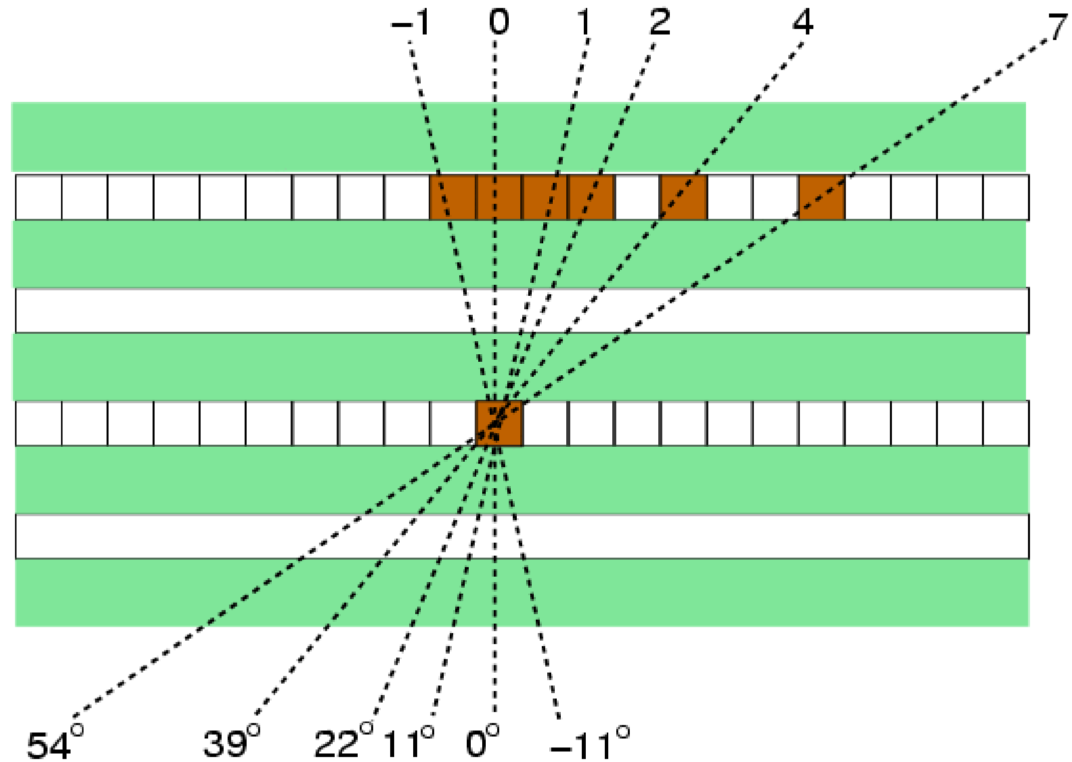

−1
0
1
2
4
7
54°
39°
22°
11°
0°
−11°

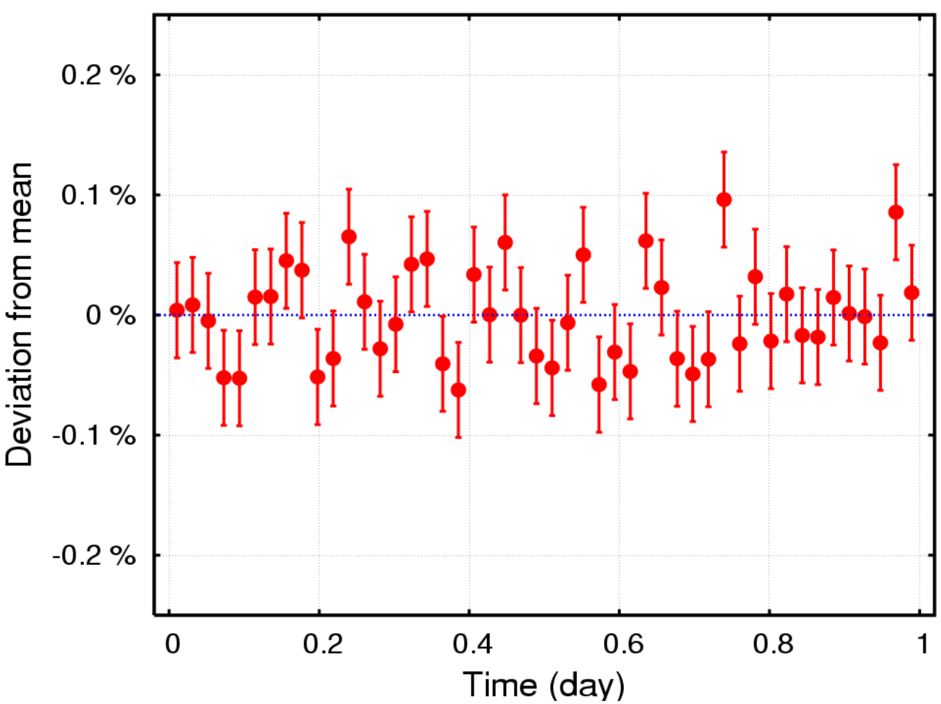

Deviation from mean
0.2 %
0.1 %
0 %
-0.1 %
-0.2 %
0
0.2
0.4
0.6
0.8
1
Time (day)

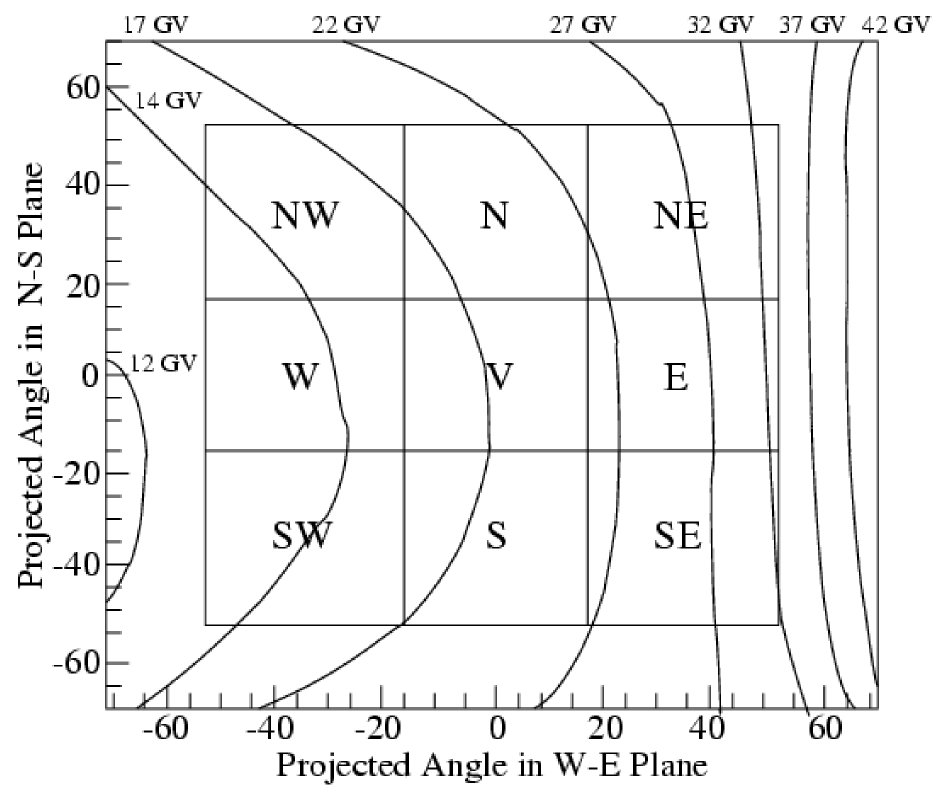

17 GV
22 GV
27 GV
32 GV
37 GV
42 GV
14 GV
12 GV
NW
N
NE
W
V
E
SW
S
SE
Projected Angle in N-S Plane
Projected Angle in W-E Plane
60
40
20
0
-20
-40
-60
-60
-40
-20
0
20
40
60

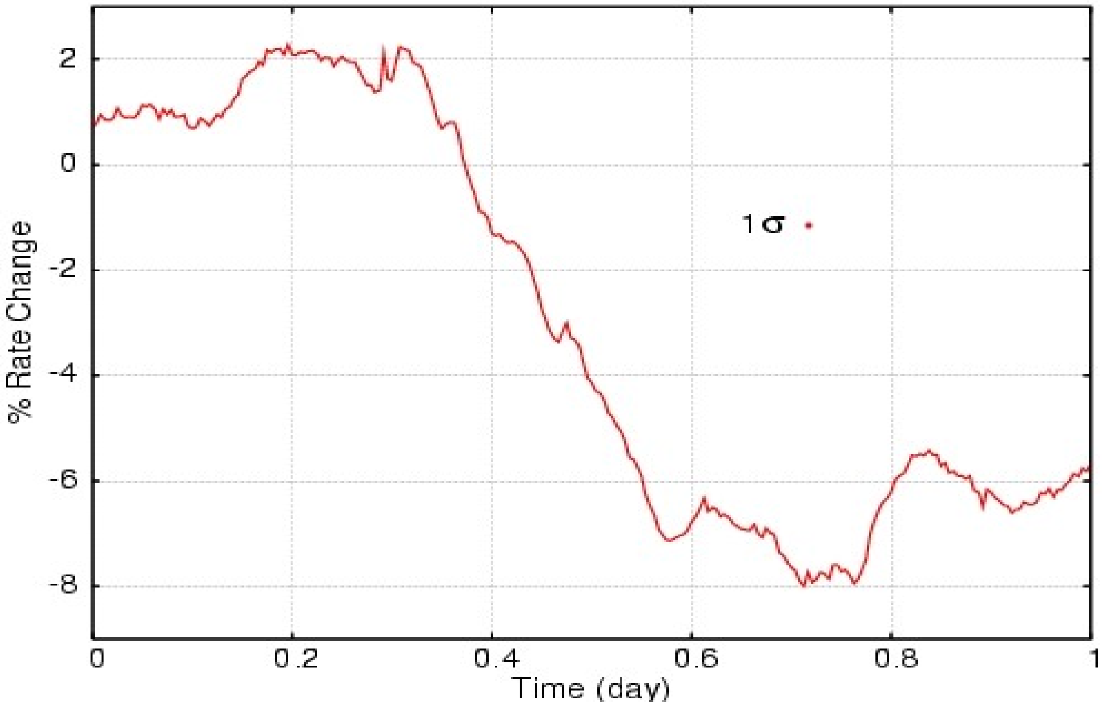

GRAPES-3

29 October 2003

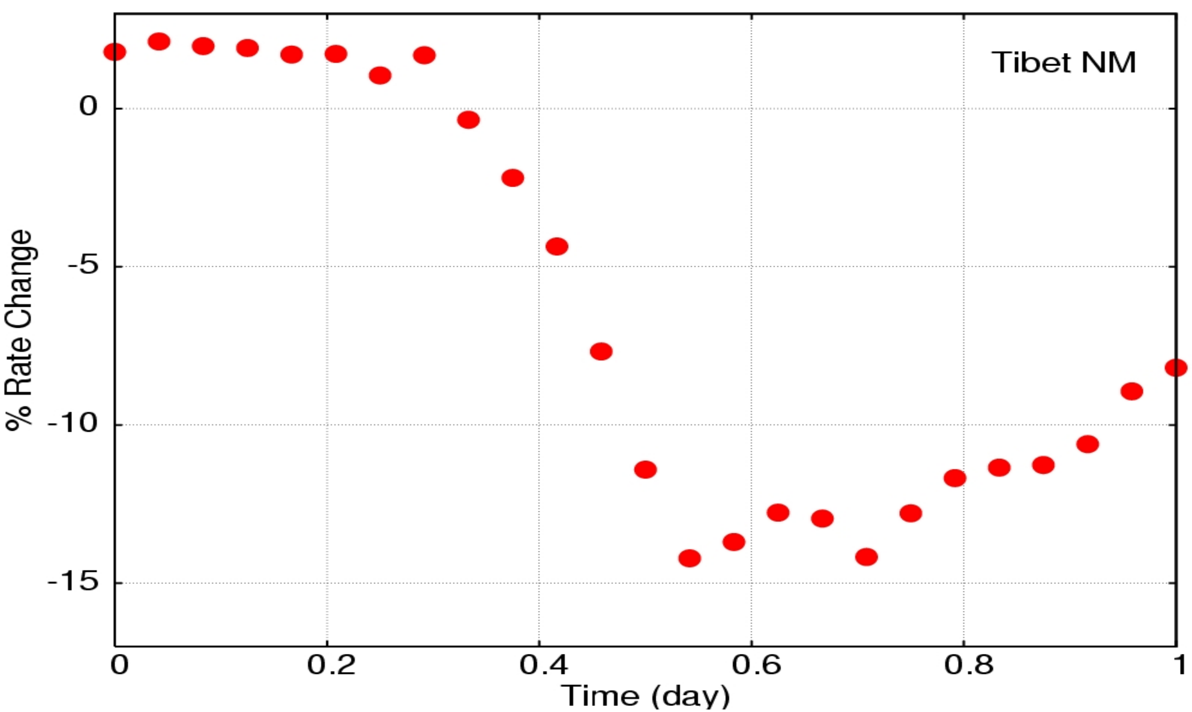

TIBET-NM

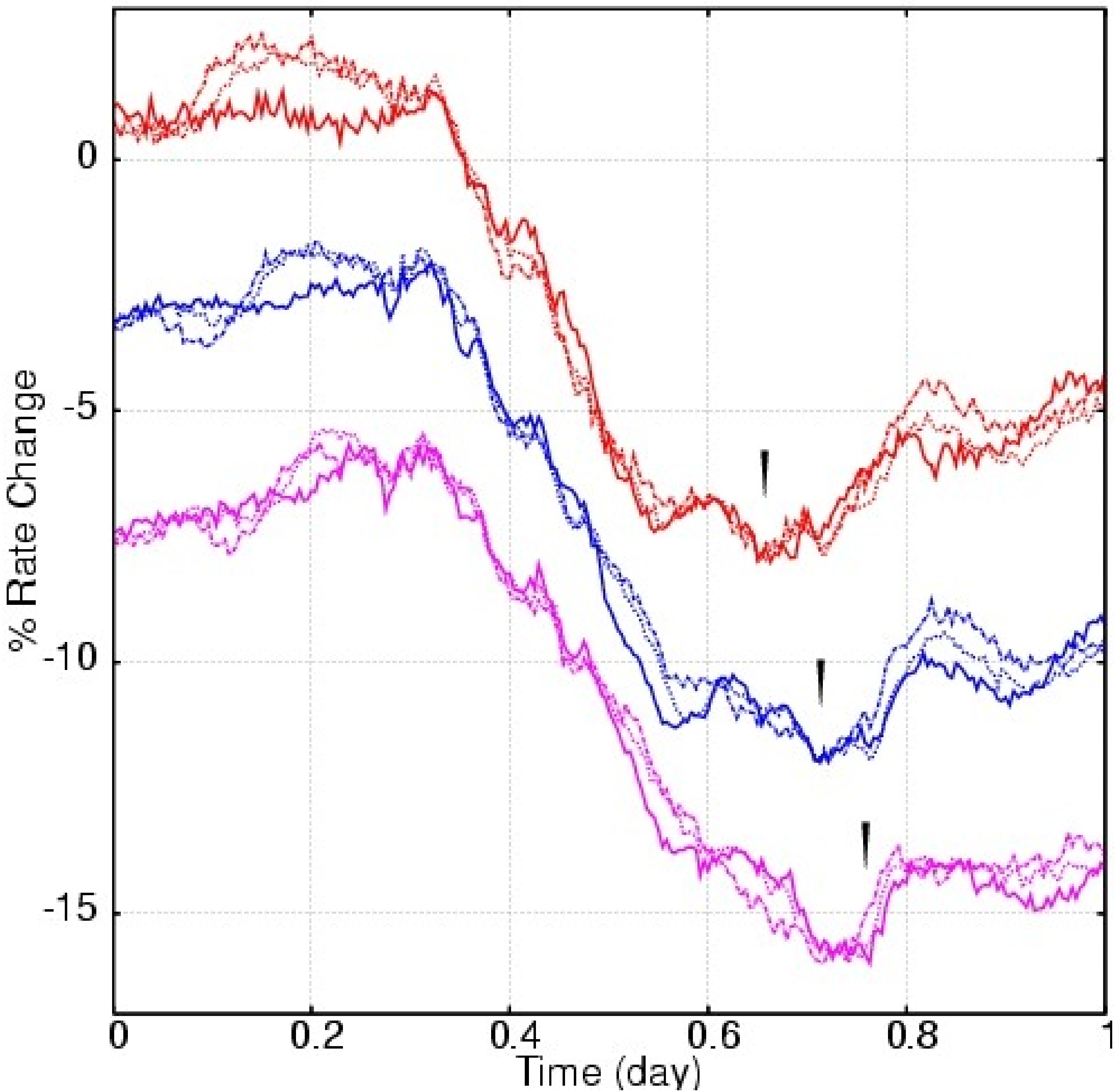

0
-5
-10
-15
% Rate Change
0
0.2
0.4
0.6
0.8
1
Time (day)

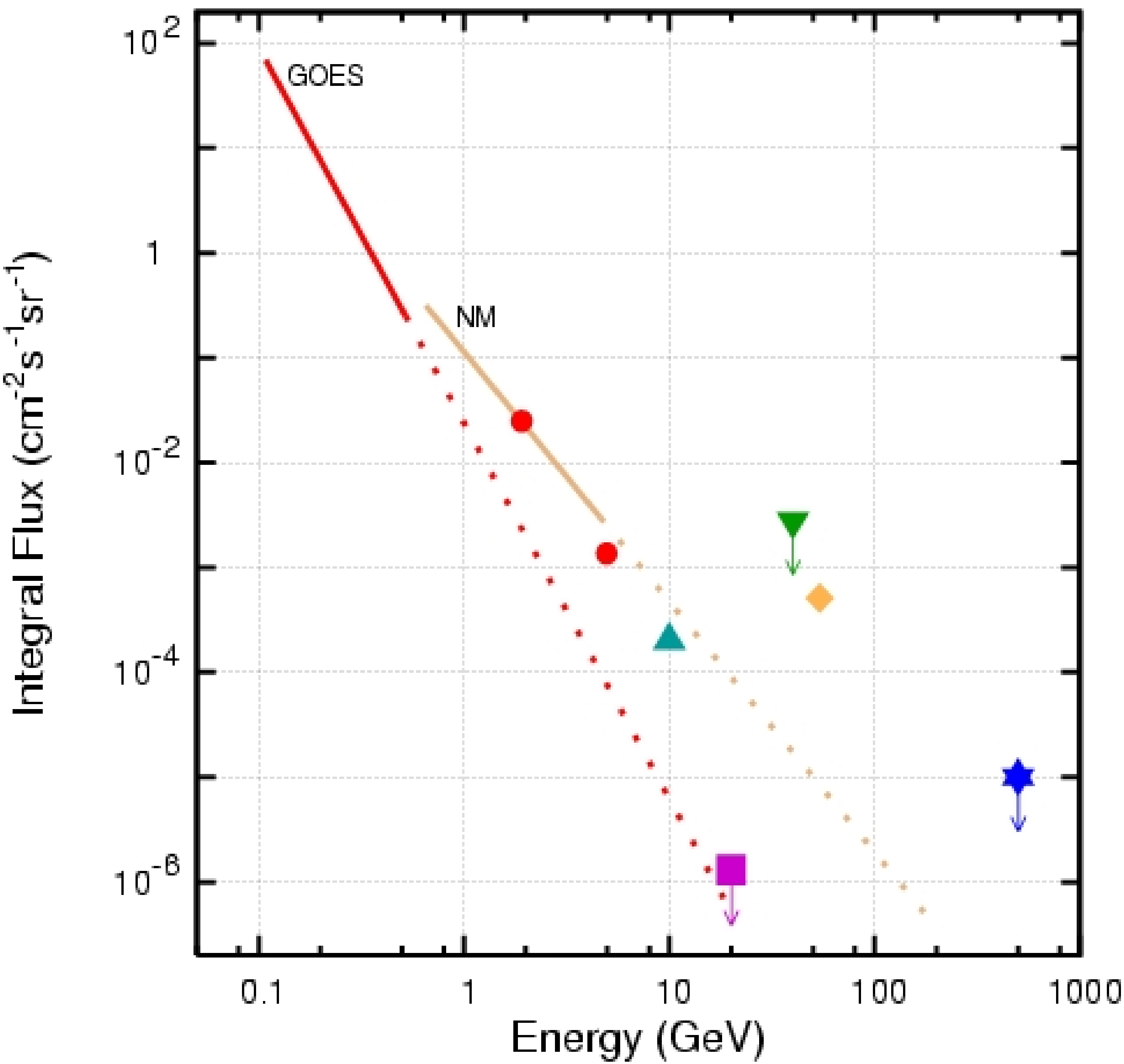
GOES
NM
Integral Flux (cm^{-2}s^{-1}sr^{-1})
10^2
1
10^{-2}
10^{-4}
10^{-6}
0.1
1
10
100
1000
Energy (GeV)

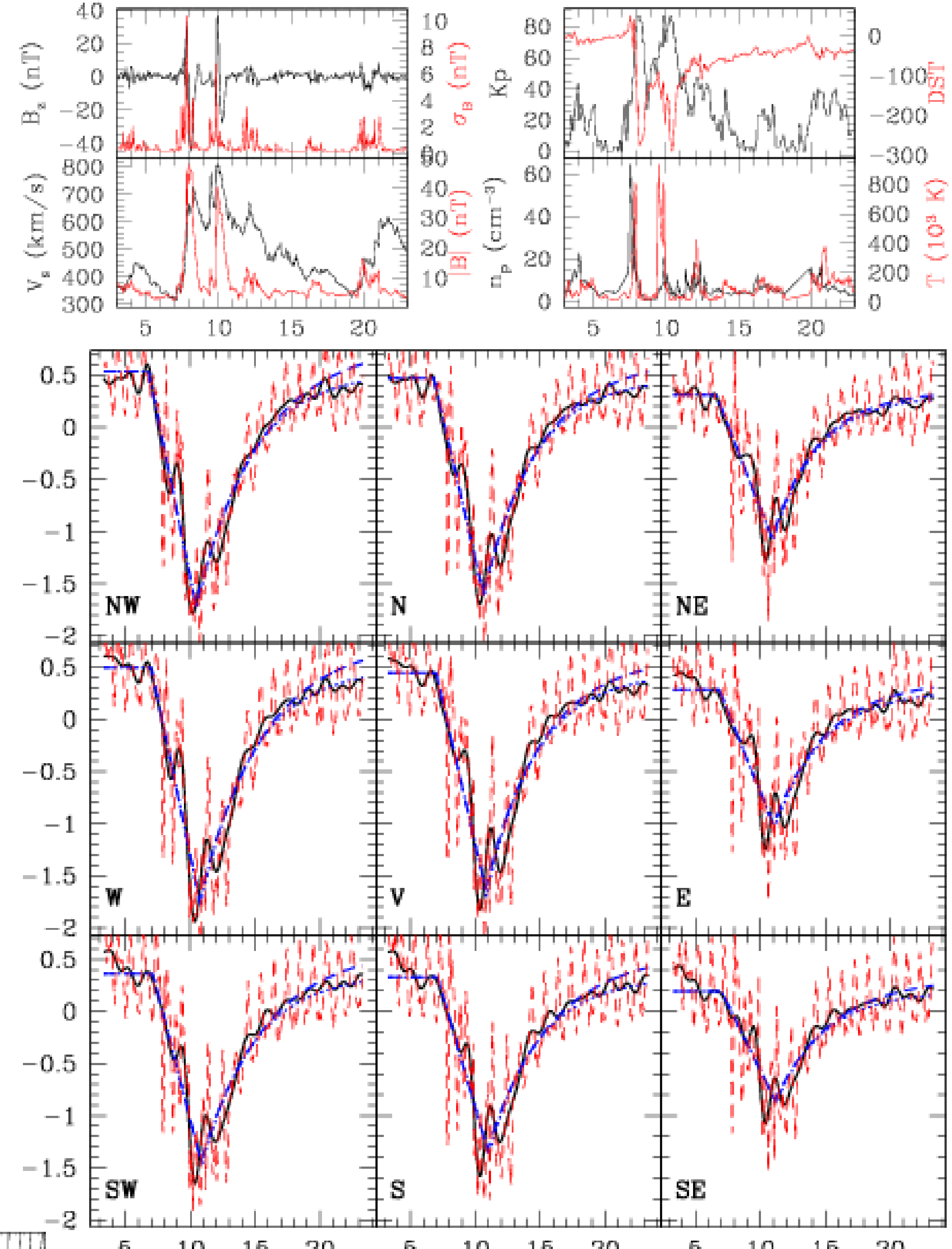

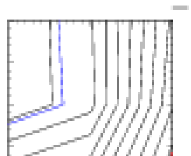

6 November 2004 21:52

CME: 11/03/16:06 (2.4×10^{31} ergs 1128 km/s Halo) &

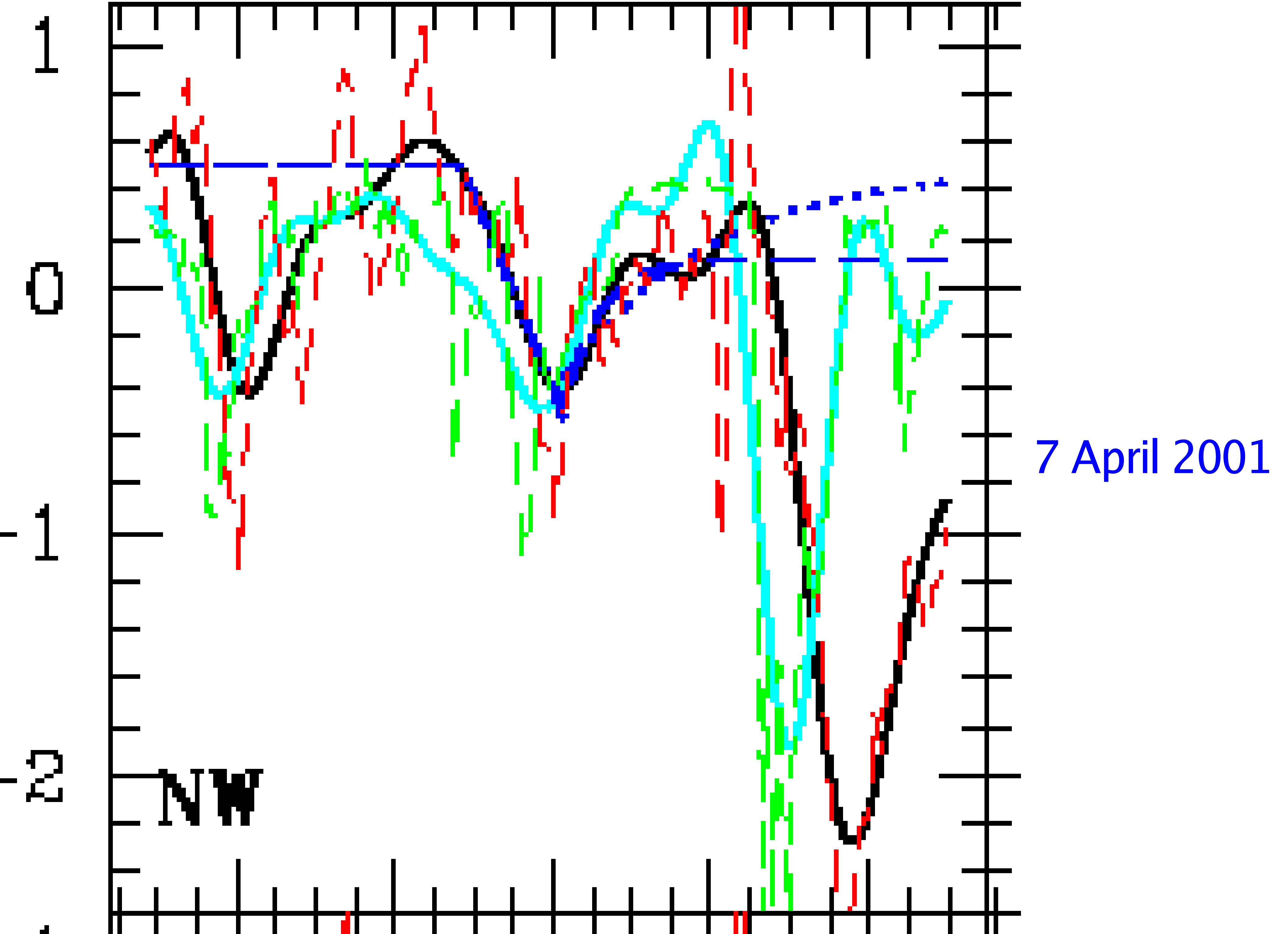

1
0
-1
-2
NW
7 April 2001

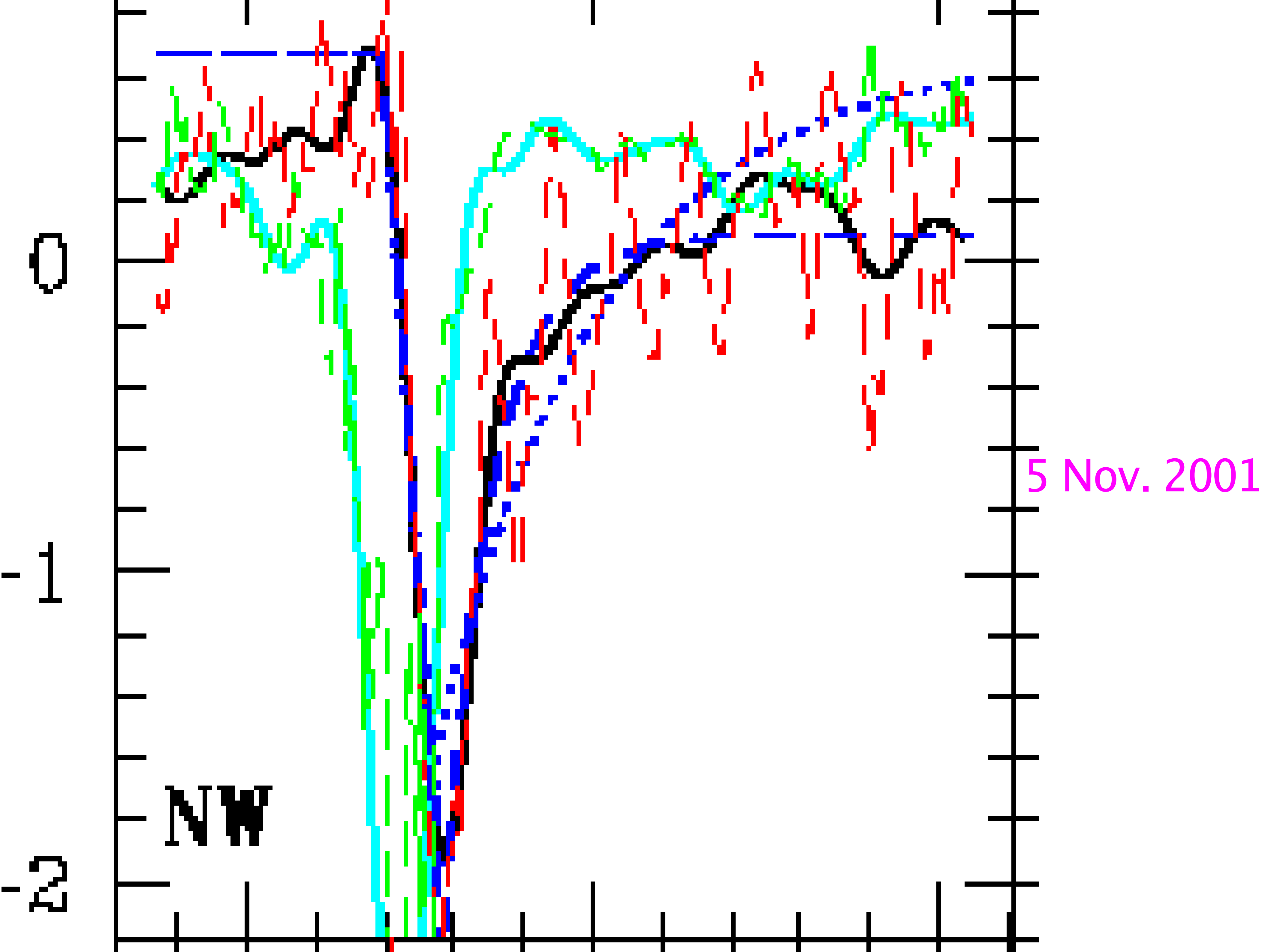

0
-1
-2
NW
5 Nov. 2001

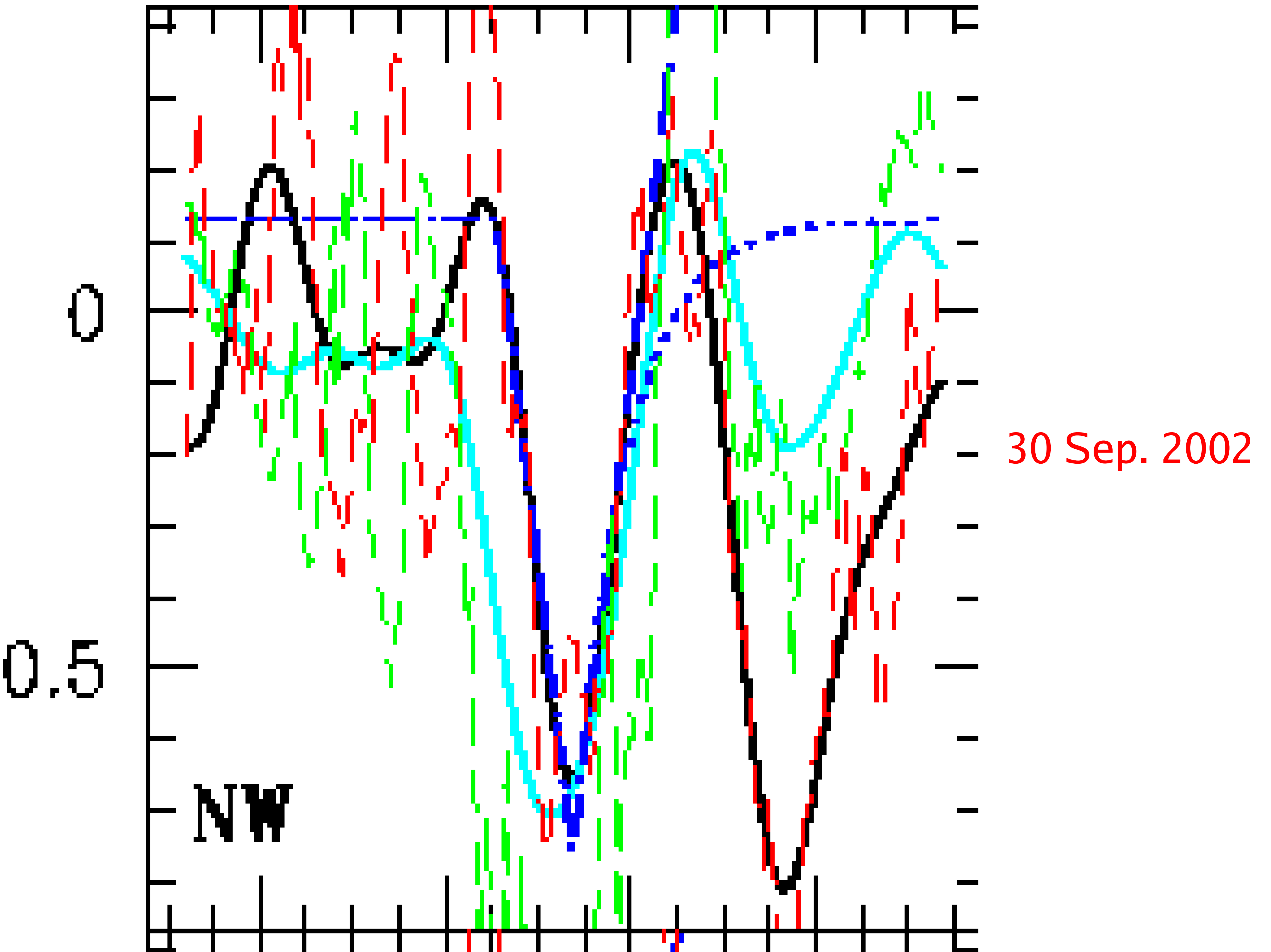
0
0.5
NW
30 Sep. 2002

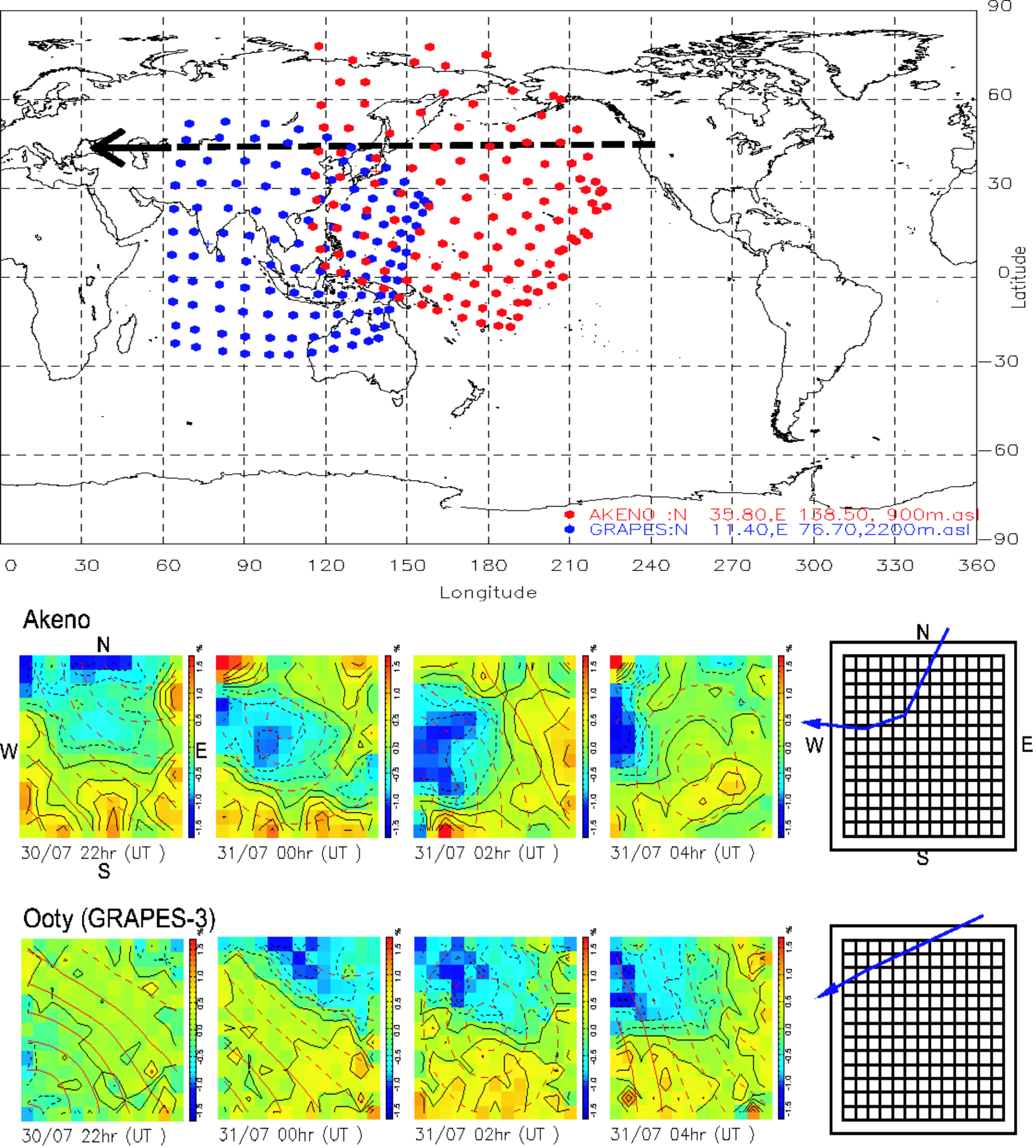
AKENO :N 35.80,E 138.50, 900m.asl
GRAPES:N 11.40,E 76.70,2200m.asl
Longitude
Latitude
Akeno
N
S
W
E
30/07 22hr (UT)
31/07 00hr (UT)
31/07 02hr (UT)
31/07 04hr (UT)
Ooty (GRAPES-3)
30/07 22hr (UT)
31/07 00hr (UT)
31/07 02hr (UT)
31/07 04hr (UT)

Future Expansion Plans

- Expansion to an area of 1 km^2 using widely spaced detectors with in-situ signal digitization
- Increase of muon detector area from 560 to 1120 m^2
- Installation of a multi-element, wide-angle, steerable Cerenkov telescope
- Installation of neutron monitors for solar studies
- Installation of low frequency dipole array for detection of radio emission from showers

Thanks

The main, naturally occurring radioactive nuclei is U^{238} which is present in the soil in very very small concentration ~1 part in 10^9. The decay chain of U^{238} results in production of other radioactive nuclei as shown below,

$$ {}_{92}U^{238} \xrightarrow[4.5\times10^9\ \text{yr}]{\alpha} {}_{90}Th^{234} \xrightarrow[24.1\ \text{day}]{\beta} {}_{91}Pa^{234} \xrightarrow[70.2\ \text{sec}]{\beta} {}_{92}U^{234} \qquad (T_{1/2}) $$

$$ {}_{92}U^{234} \xrightarrow[2.5\times10^5\ \text{yr}]{\alpha} {}_{90}Th^{230} \xrightarrow[7.5\times10^4\ \text{yr}]{\alpha} {}_{88}Ra^{226} \xrightarrow[1600\ \text{yr}]{\alpha} {}_{86}Rn^{222} \qquad (T_{1/2}) $$

Daughter product of U^{238} is Rn^{222} a gas, that escapes from the soil into the atmosphere where it mixes in the air due to its half-life of 3.82 days, before decaying into Po^{218}. The decay chain of Rn^{222} is schematically shown below. Radon daughter products are heavy metals are precipitated along with rain-fall. The radon daughter nuclei Pb^{214} ($T_{1/2}$=26.8 minutes) and Bi^{214} ($T_{1/2}$=19.9 minutes) are the two most important radioactive nuclei,

$$ {}_{86}Rn^{222} \xrightarrow[3.8\ \text{day}]{\alpha} {}_{84}Po^{218} \xrightarrow[3.1\ \text{min}]{\alpha} {}_{82}Pb^{214} \xrightarrow[26.8\ \text{min}]{\beta} {}_{83}Bi^{214} \qquad (T_{1/2}) $$

$$ {}_{83}Bi^{214} \xrightarrow[19.9\ \text{min}]{\beta} {}_{84}Po^{214} \xrightarrow[164\ \mu s]{\alpha} {}_{82}Pb^{210} \xrightarrow[22.2\ \text{yr}]{\beta} {}_{83}Bi^{210} \qquad (T_{1/2}) $$

$$ {}_{83}Bi^{210} \xrightarrow[5.01\ \text{day}]{\beta} {}_{84}Po^{210} \xrightarrow[138.4\ \text{day}]{\alpha} {}_{82}Pb^{206} \qquad (T_{1/2}) $$

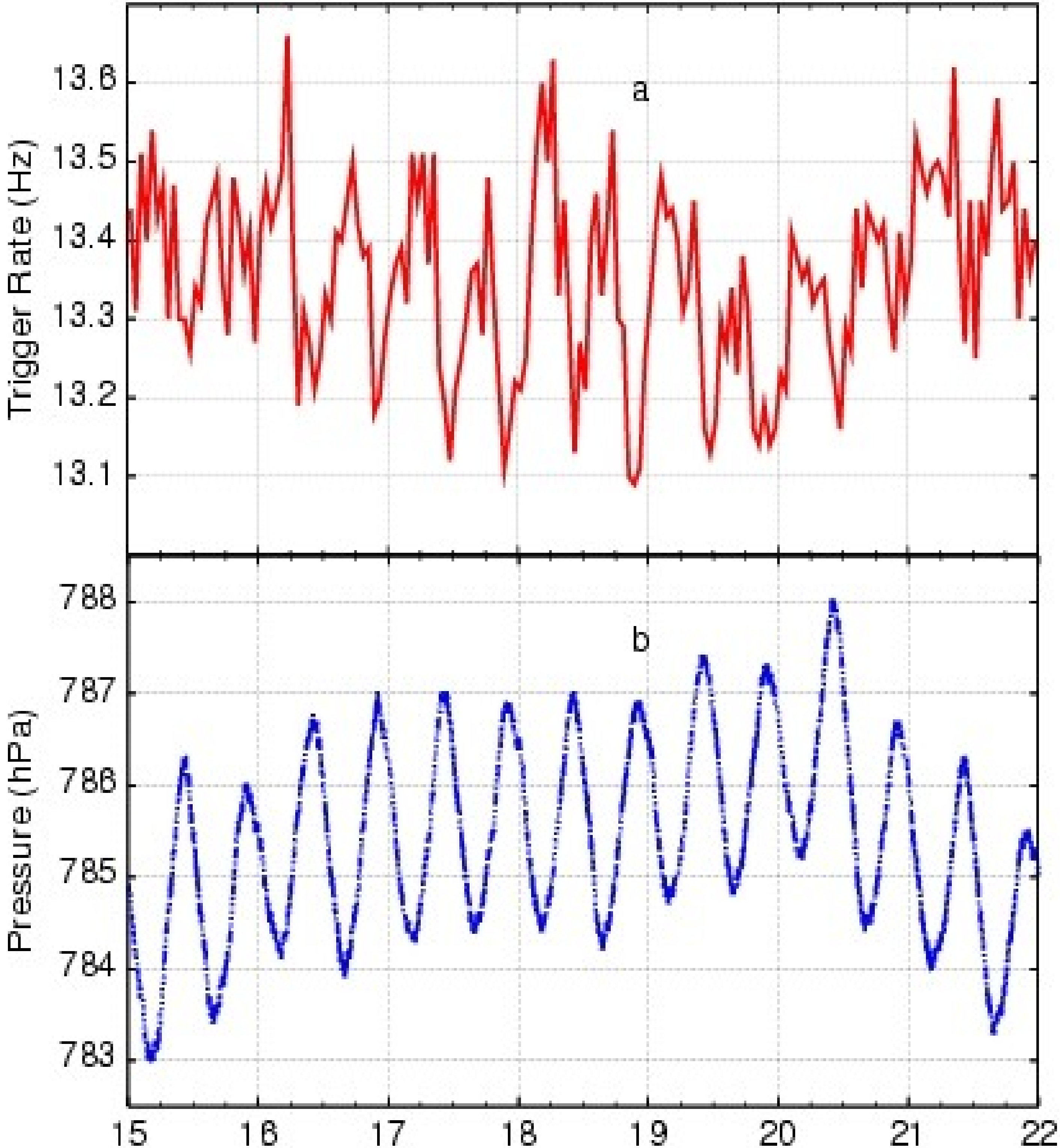

a
b
Trigger Rate (Hz)
Pressure (hPa)
13.6
13.5
13.4
13.3
13.2
13.1
788
787
786
785
784
783
15
16
17
18
19
20
21
22

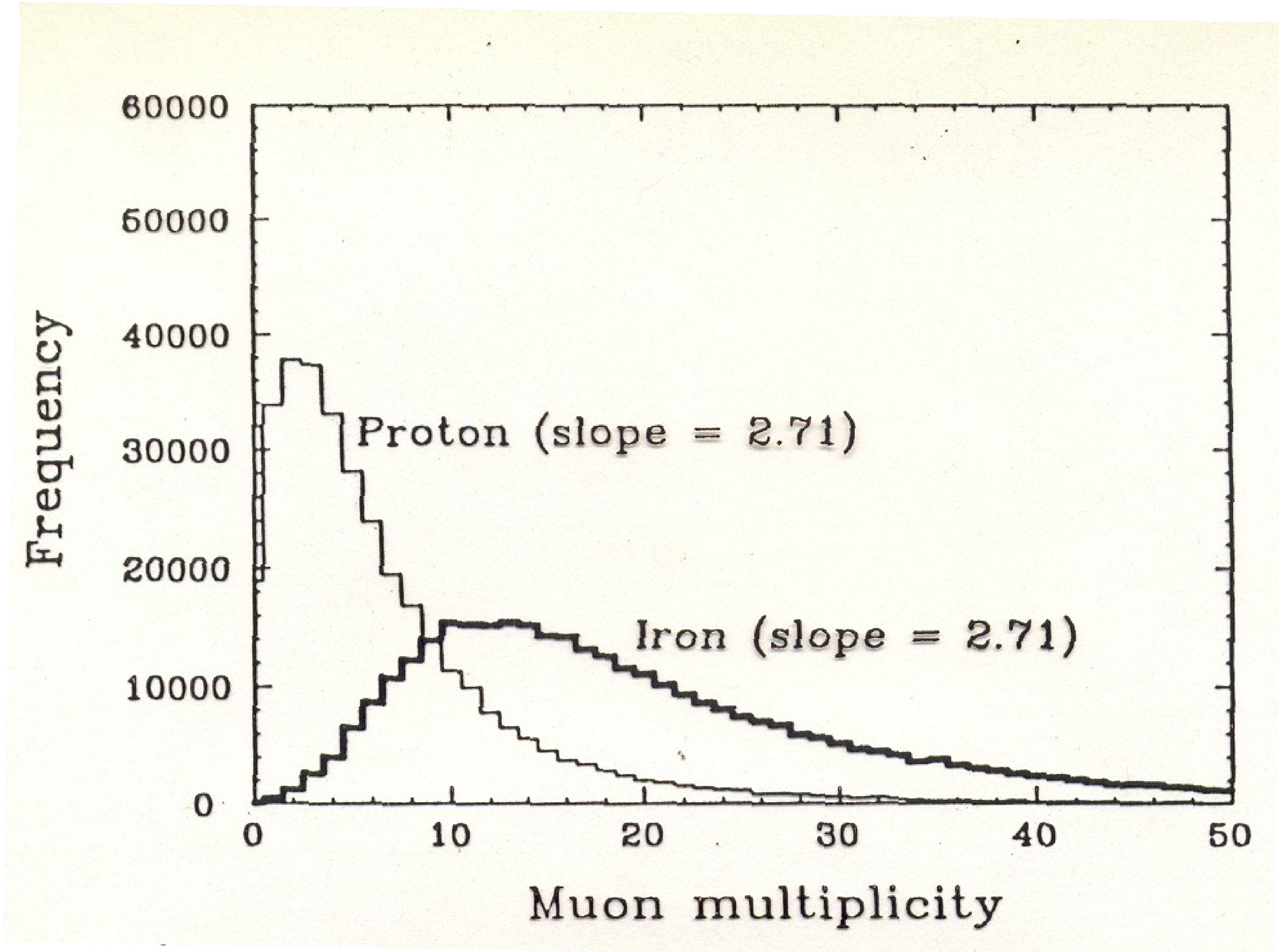

Comparison of muon multiplitcity distributions for showers initiated by protons and Fe nuclei, simulated assuming the same value of 2.71 for the spectral index

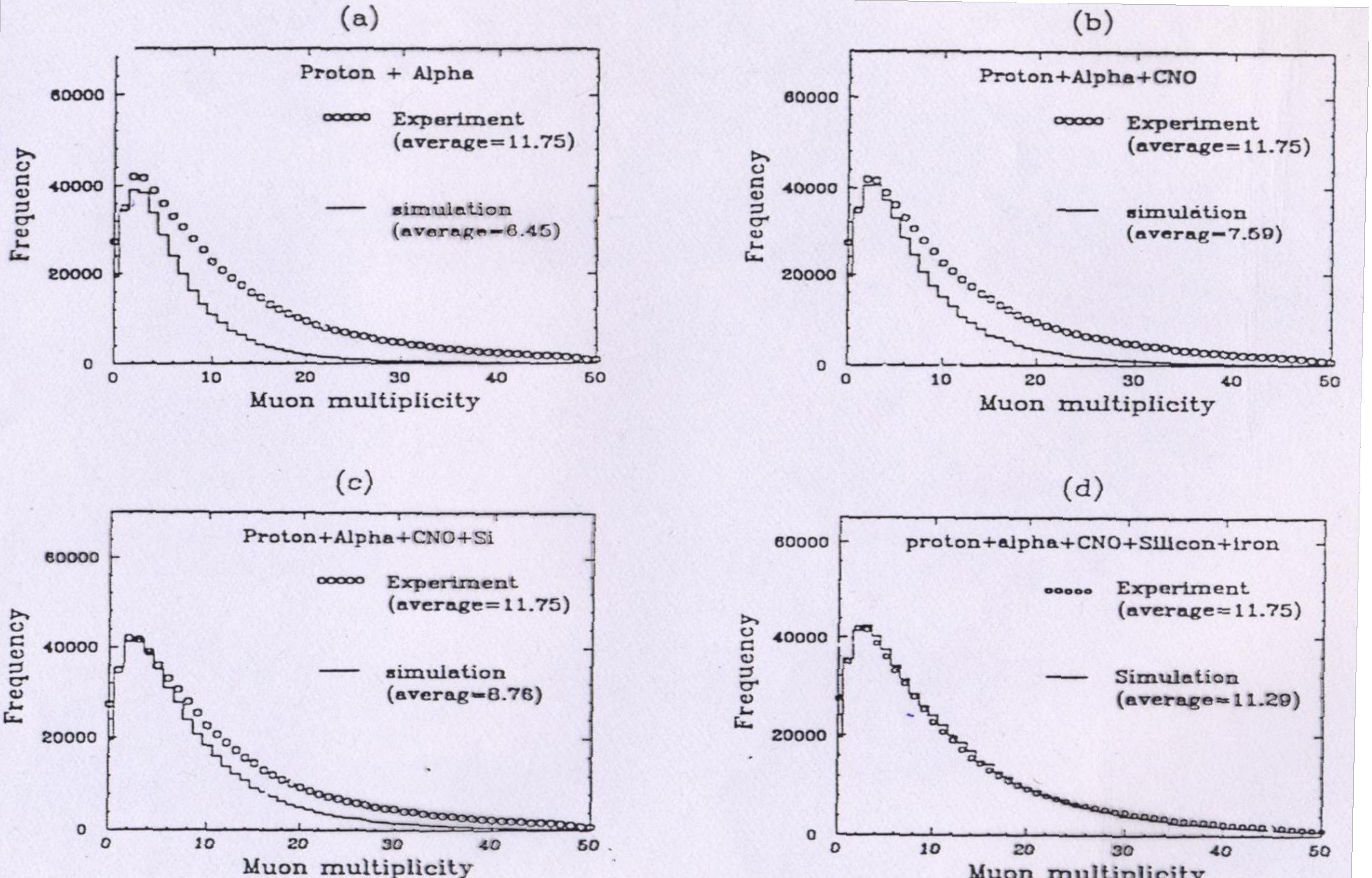

Figure 5.21: Incremental contributions of different primary nuclear groups to different regions of the *muon multiplicity distribution* obtained from simulations for the *Ooty composition* model.

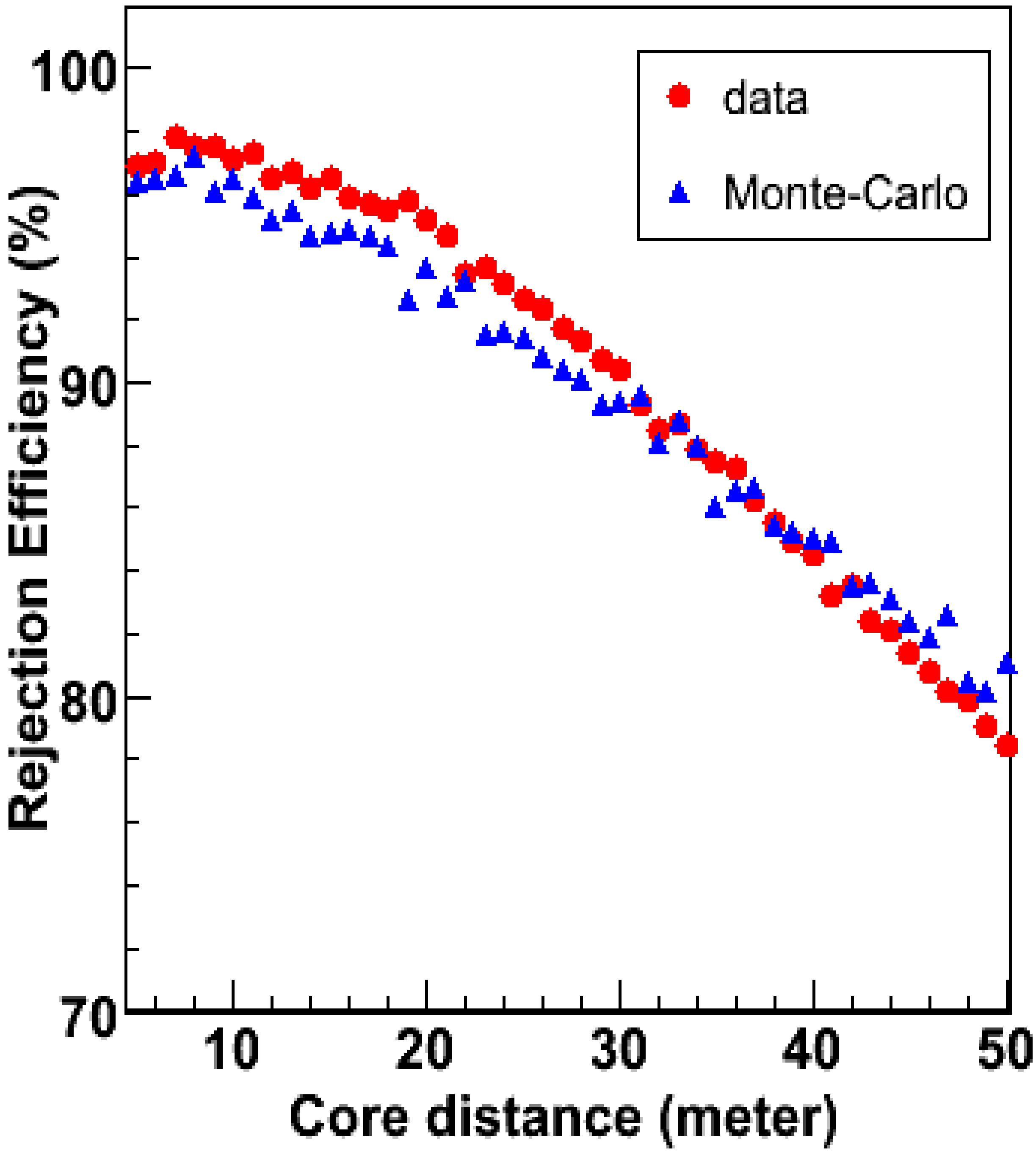

data
Monte-Carlo
Rejection Efficiency (%)
100
90
80
70
10
20
30
40
50
Core distance (meter)

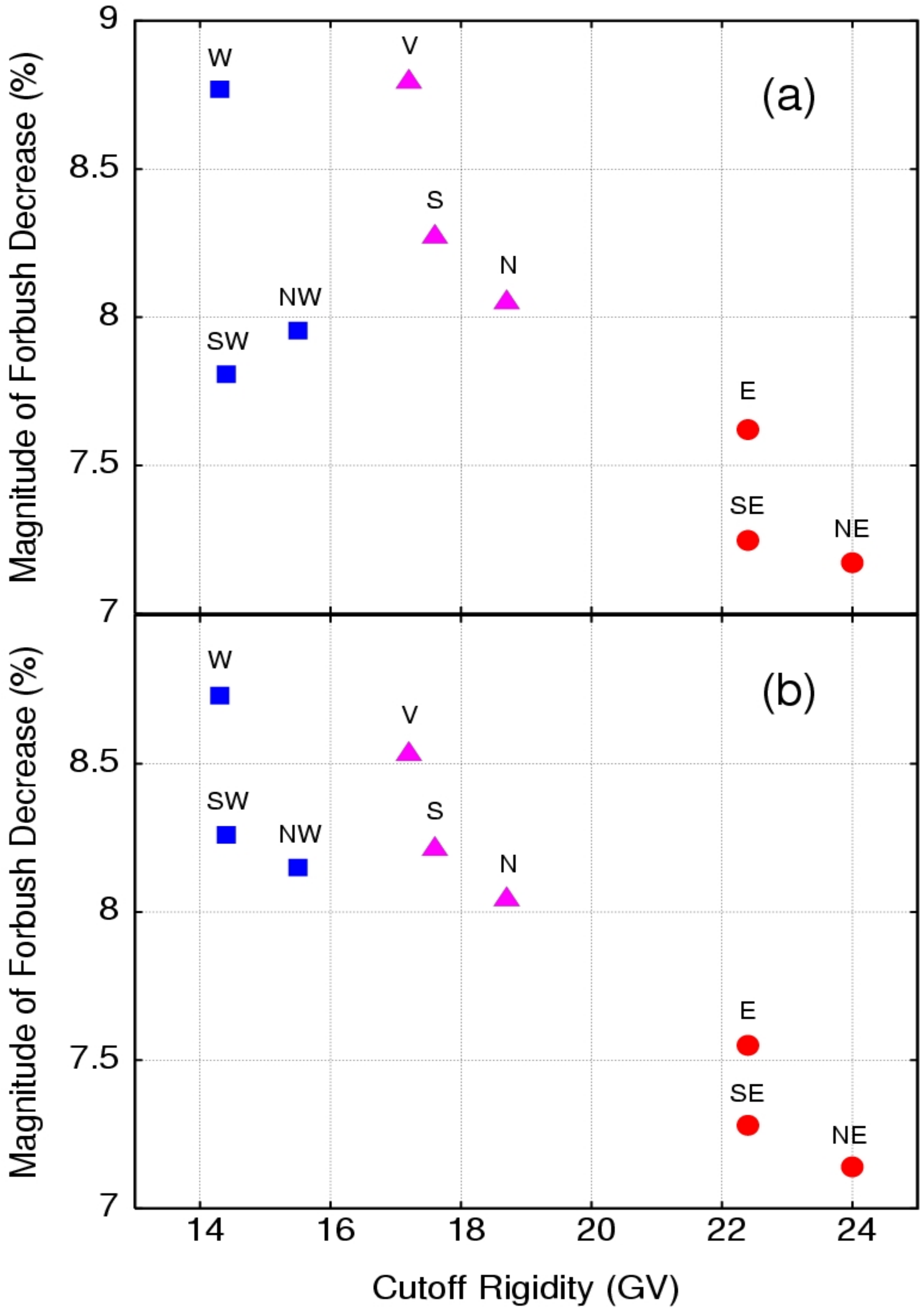

- $A(r) = K \times r^{-\gamma}$
- $K = (12.3 \pm 0.3)\%$
- $\gamma = (0.53 \pm 0.04)$
- $\gamma = 0.4 - 1.2$

Future Goals:

1. Precision measurement of nuclear composition and energy spectrum from $3x10^{13}$ to $3x10^{18}$ eV encompassing the region which includes the direct measurements, “knee” and “ankle” in a single experiment with electron and muon and Cerenkov detection.

This information is essential for understanding the origin of cosmic rays, the nature of acceleration processes and the properties of the interstellar medium in which they propagate prior to detection at Earth.

2. Pin down the ratio of the diffused γ-rays and protons above 100 TeV produced by $>10^{20}$ eV particles. This should clarify if the non-conventional models based on topological defects can explain the highest energy particles.

3. Precision measurements of the energetic solar particles to determine the sites and mechanisms for acceleration. Studies of Sun induced phenomena such as CMEs and Forbush decrease etc. having implications on space-weather.

4. High sensitivity search for point source of γ-rays above 100 TeV from neutron stars, black holes and other compact sources.

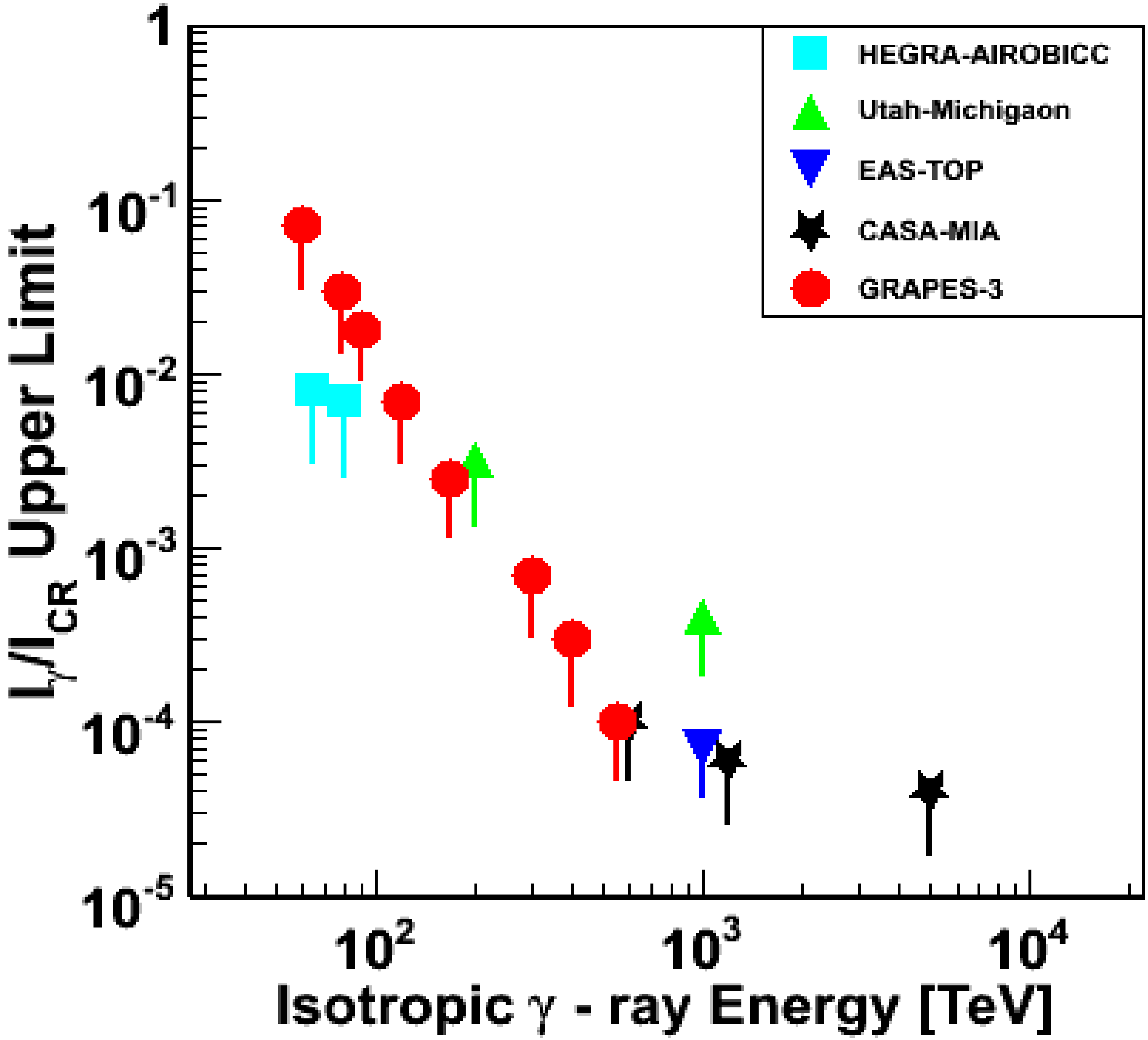
HEGRA-AIROBICC
Utah-Michigaon
EAS-TOP
CASA-MIA
GRAPES-3
I_γ/I_{CR} Upper Limit
1
10^{-1}
10^{-2}
10^{-3}
10^{-4}
10^{-5}
10^{2}
10^{3}
10^{4}
Isotropic γ - ray Energy [TeV]


2007
44